

Recent Advances in Quartz-Enhanced Photoacoustic Spectroscopy for Gas Sensing Applications

Presented by:





Technical Group Leadership:

Krishnan Parameswaran, Analog Devices Inc., USA

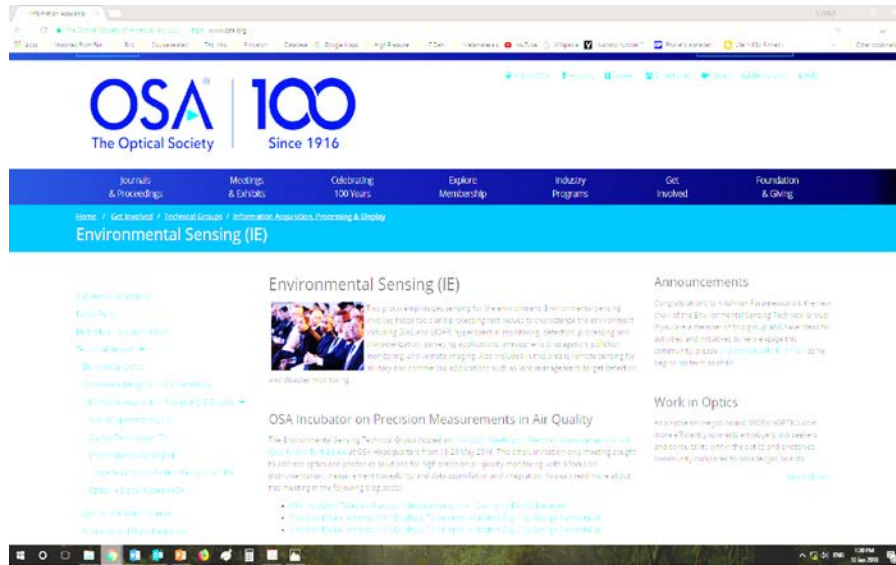
Joachim Sacher, Sacher Lasertechnik GmbH, Germany

Amartya Sengupta, Indian Institute of Technology Delhi, India



Technical Group Website:

www.osa.org/EnvironmentalSensingTG



Over 1,100 Total Members

Scope:

This technical group covers optical tools and techniques used in environmental sensing, including DIAL and LIDAR, hyperspectral monitoring, detection, processing and characterization, surveying applications, atmospheric propagation, pollution monitoring, and remote imaging. Also included in this area is remote sensing for military and commercial applications such as land management, target detection, and disaster monitoring.

Contact your Technical Group and Get Involved!

www.linkedin.com/groups/12055528

OSA Environmental Sensing Technical Group
72 members

Start a conversation with your group

Enter a conversation title...

[Conversations](#) [Jobs](#)

Krishnan Parameswaran · Moderator
Photonics Engineering Manager at Analog Devices

Webinar! Volcanoes!

Hello All. I am happy to announce the first OSA Environmental Sensors Webinar of 2018. The exciting topic is Remote Sensing of Volcanoes using Smart Sensing Technology.

Here are the details

Presenter: Dr. Andrew McGonigle, University of Sheffield
Date: Wednesday January 17, 2018
Time: 1000 Eastern Time (United States), 1500 GMT

Registration Link: <https://cc.callinfo.com/registration/#/?meeting=1ee274c1e6be&campaign=1b7e6d4e180f>

- **Linked-In site**
- **Announce new activities**
- **Promote interactions**
- **Complement our OSA Technical Group Member Listserv**
- **Activities: Webinars, Special Sessions in CLEO/FiO**

OSA INCUBATORS

Collaborate. Innovate. Discover.



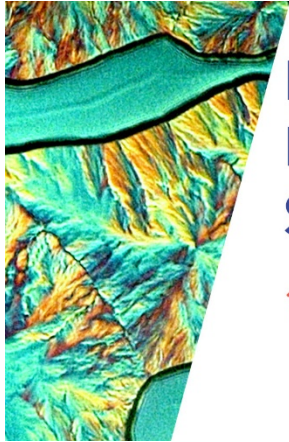
OSA Agri-Photonics Incubator Advanced Spectroscopy in Precision Agriculture

12-14 May 2019, OSA Headquarters, Washington DC

We are excited to share with you that our technical group has been working on planning an OSA Incubator focused on exploring advanced spectroscopy in precision agriculture. Visit www.osa.org/agriphotonicsinc to learn more!



Welcome to Today's Webinar!



RECENT ADVANCES IN QUARTZ-ENHANCED
PHOTOACOUSTIC SPECTROSCOPY FOR GAS
SENSING APPLICATIONS

18 February 2019 • 10:00 EST



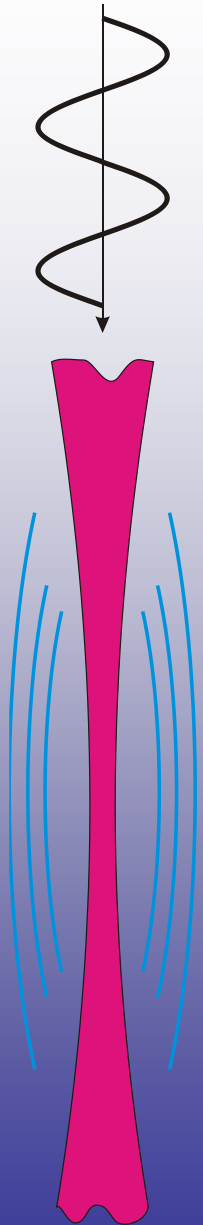
Vincenzo Spagnolo obtained the PhD in physics in 1994 from University of Bari. From 1997 to 1999, he worked as researcher of the National Institute of the Physics of Matter (INFM). Since 2004, he has been with the Technical University of Bari, formerly as assistant and associate professor and, starting from 2018, as Full Professor of Applied Physics. He is “Hundred Talent” visiting professor as Shanxi University in Taiyuan (China). He is the director of the joint-research lab PolySense created by Technical University of Bari and THORLABS GmbH. His research interests include optoacoustic gas sensing and spectroscopic techniques for real-time device monitoring. His research activity is documented by more than 180 Scopus publications and two filed patents. He has given more than 50 invited/keynote presentations at international conferences and workshops. Prof. Spagnolo is program committee member of several SPIE and OSA conferences. He is editor of Sensors (MPDI), Applied Science (MPDI) and Journal of Sensors (Hindawi). Prof. Spagnolo is senior member of the OSA and senior member of SPIE.

Recent advances in quartz-enhanced photoacoustic spectroscopy for gas sensing applications

Vincenzo Spagnolo

PolySense Lab, Technical University of Bari – Italy

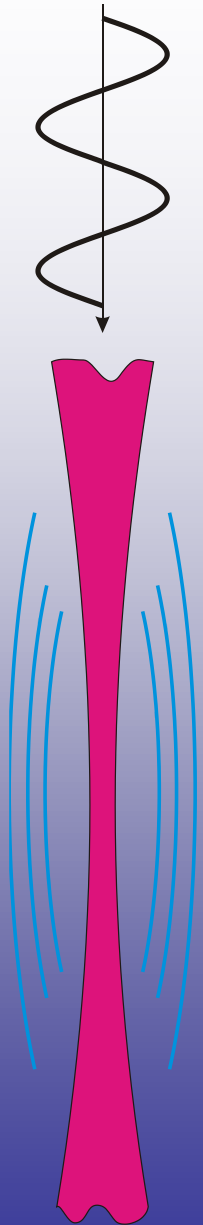
- Motivation for optical Gas Sensing
- Quartz Enhanced Photoacoustic gas detection



Recent advances in quartz-enhanced photoacoustic spectroscopy for gas sensing applications

Vincenzo Spagnolo

PolySense Lab, Technical University of Bari – Italy



- Motivation for optical Gas Sensing
- Quartz Enhanced Photoacoustic gas detection
 - QEPAS: Basic principles and merits
 - QEPAS with custom quartz tuning forks
 - QEPAS in the THZ range
 - Intracavity QEPAS
 - Real word applications
- Future perspectives

Main applications of gas sensing

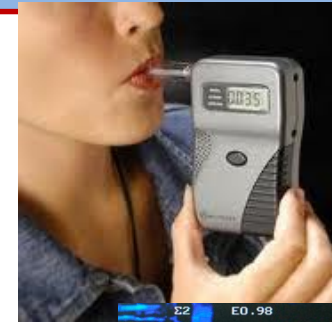
Industrial process control

- Chemical analysis
- Monitoring combustion processes
- Quantification of gas leaks



Health and Life Sciences

- Breath analysis
- Biomedicine



TRACE GAS SENSING APPLICATIONS

Environmental Monitoring

- Air pollution monitoring
- Detection of toxic gases
- Eco-sustainability

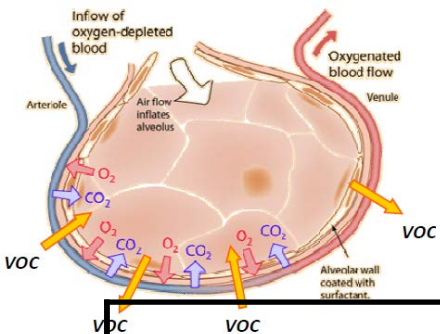
Law Enforcement

- National Security
- Defense



Trace gases in the atmosphere

Chemical species		Concentration	Residence time	Sources					
Name	Formula			Biogenic	Anthropogenic	Photochemical	Volcanic	Radiogenic	Other
Nitrogen	N ₂	78.084%	1.6×10 ⁷ years	✓			✓		
Oxygen	O ₂	20.946%	3×10 ³ –10 ⁴ years	✓					
Argon	Ar	0.934%						✓	
Water vapour*	H ₂ O	0–4% (0– 40 000 ppm)	10 days	✓	✓		✓		(1)
Carbon dioxide	CO ₂	3.94×10 ⁻² % (394 ppm)	20–150 years	✓	✓		✓		
Neon	Ne	1.818×10 ⁻³ % (18.18 ppm)					✓?		
Helium	He	5.24×10 ⁻⁴ % (5.24 ppm)	10 ⁷ years					✓	
Methane	CH ₄	1.79×10 ⁻⁴ % (1.79 ppm)	10 years	✓	✓				
Krypton	Kr	1.14×10 ⁻⁴ % (1.14 ppm)						✓	
Hydrogen	H ₂	5.3×10 ⁻⁵ % (0.53 ppm)	2 years	✓	✓				(2)
Nitrous oxide	N ₂ O	3.25×10 ⁻⁵ % (0.325 ppm)	150 years	✓	✓				
Carbon-monoxide	CO	5–25×10 ⁻⁶ % (0.05–0.25 ppm)	0.2–0.5 year	✓	✓				
Xenon	Xe	8.7×10 ⁻⁶ % (0.087 ppm)							
Ozone	O ₃	1–5×10 ⁻⁶ % (0.01–0.05 ppm)	weeks - months			✓			
Nitrogen-dioxide	NO ₂	0.1–5×10 ⁻⁷ % (0.001–0.05 ppm)	8–10 days	✓	✓	✓			
Ammonia	NH ₃	0.01–1×10 ⁻⁷ % (0.0001–0.01 ppm)	~5 days	✓	✓				
Sulphur-dioxide	SO ₂	0.003–3×10 ⁻⁷ % (0.03–30×10 ⁻³ ppm)	~2 days		✓	✓	✓		
Hydrogen-sulphide	H ₂ S	0.01–6×10 ⁻⁸ % (0.01–0.6×10 ⁻³ ppm)	~0.5 day	✓	✓		✓		

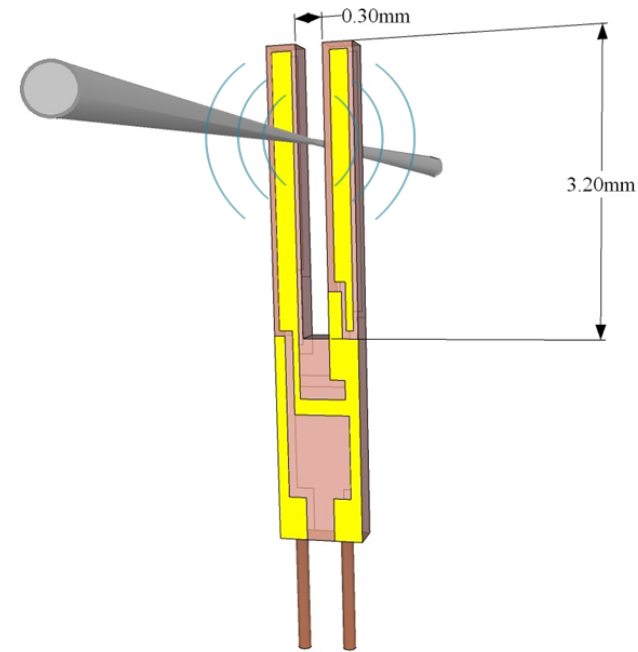


Trace gases in human breath

Molecule	Formula	Biological/Pathology Indication	Center wavelength [μm]
Pentane	C_5H_{12}	Inflammatory diseases, transplant rejection	6.8
Ethane	C_2H_6	Lipid peroxidation and oxidation stress, lung cancer (low ppbv range)	6.8
Carbon Dioxide isotope ratio	$^{13}CO_2/^{12}CO_2$	Helicobacter pylori infection (peptic ulcers, gastric cancer)	4.4
Carbonyl Sulfide	COS	Liver disease, acute rejection in lung transplant recipients (10-500 ppbv)	4.8
Carbon Disulfide	CS_2	Disulfiram treatment for alcoholism	6.5
Ammonia	NH_3	Liver and renal diseases, exercise physiology	10.3
Formaldehyde	CH_2O	Cancerous tumors (400-1500 ppbv)	5.7
Nitric Oxide	NO	Nitric oxide synthase activity, inflammatory and immune responses (e.g. asthma) and vascular smooth muscle response (6-100 ppb)	5.3
Hydrogen Peroxide	H_2O_2	Airway inflammation, oxidative stress (1-5 ppbv)	7.9
Carbon Monoxide	CO	Smoking response, lipid peroxidation, CO poisoning, vascular smooth muscle response	4.7
Ethylene	C_2H_4	Oxidative stress, cancer	10.6
Acetone	C_3H_6O	Ketosis, diabetes mellitus	7.3

OUTLINE

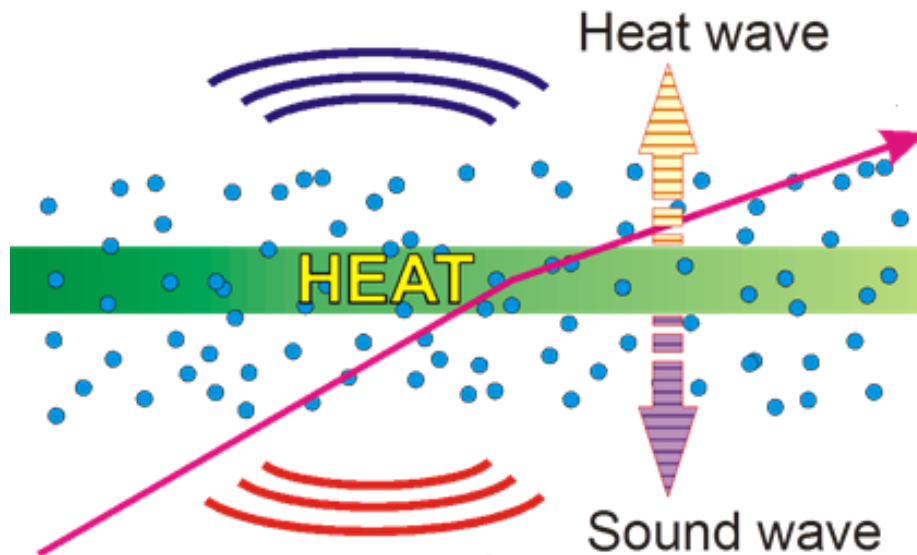
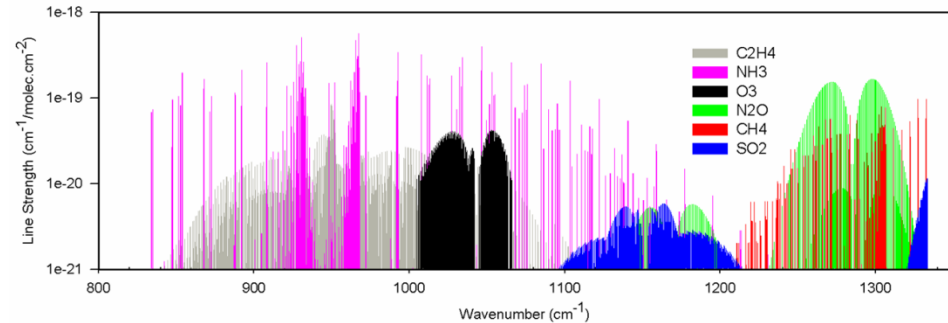
- Motivation for Gas Sensing
- Quartz Enhanced Photoacoustic (QEPAS) trace gas detection
 - Basic principles and merits
 -



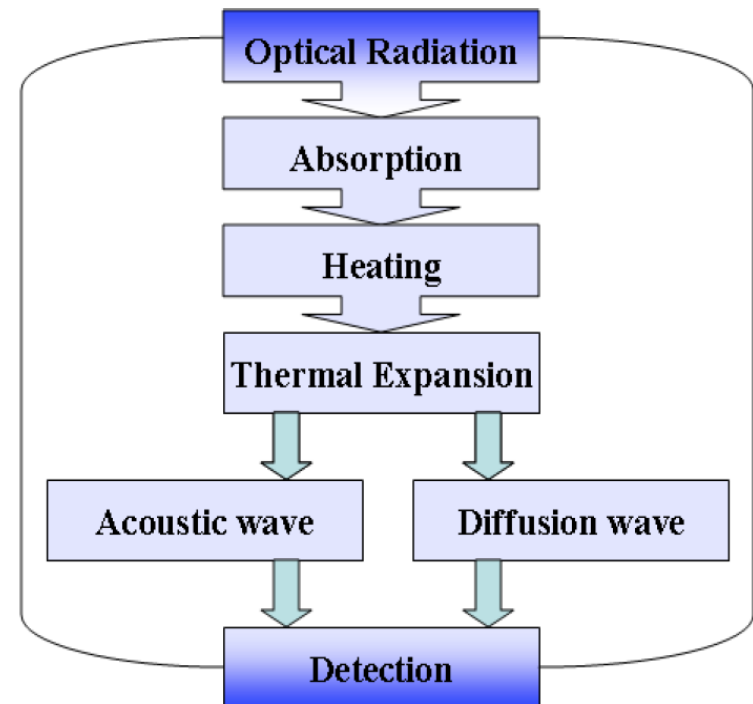
The physics of *opto-acoustic/thermal* trace gas detection

The detection of trace gases is based on the interaction between

- **optical radiation**: a laser source
- **gas molecules**: absorb light only at certain wavelengths



Photoacoustic Spectroscopy (PAS)

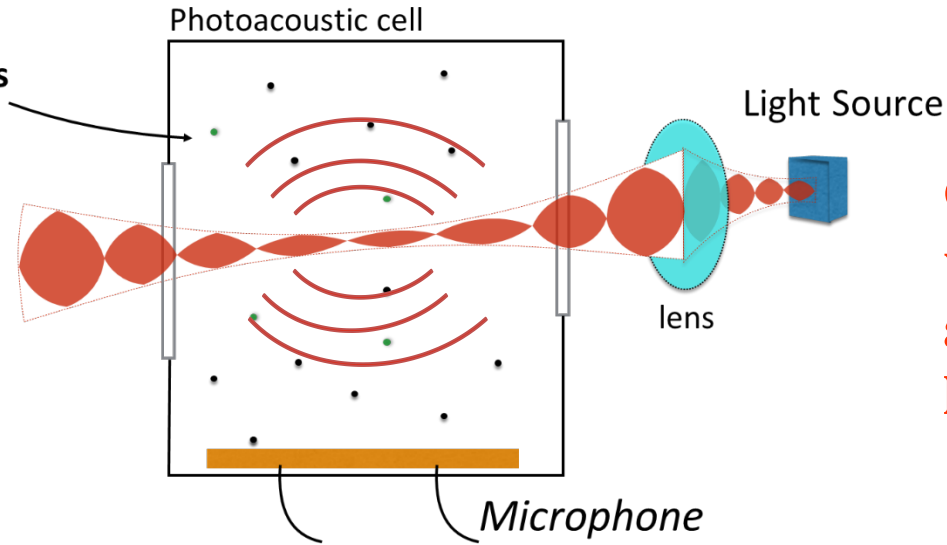


Optoacoustic Detection

The PA effect - Principle

Alexander Bell, 1880

Generation of an acoustic wave in a sample due to the absorption of a modulated laser beam



$$S = C \times P \times \alpha$$

$$\alpha = N\sigma c$$

S = photoacoustic signal

C = Instrumental constant

P = (laser) power

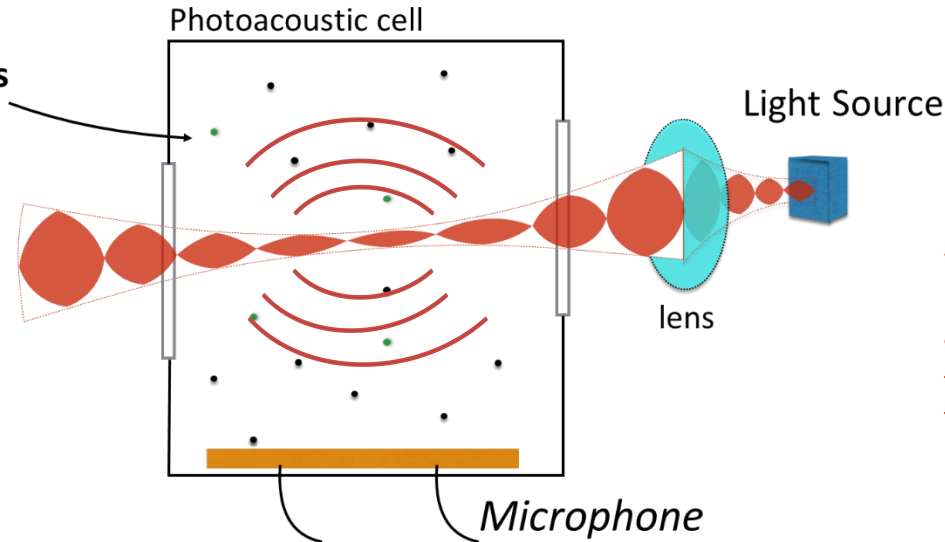
α = Absorption coefficient

→ the intensity of the sound is proportional to the concentration of absorbing molecules

The PA effect - Principle

Alexander Bell, 1880

Generation of an acoustic wave in a sample due to the absorption of a modulated laser beam



$$S = C \times P \times \alpha$$

$$\alpha = N\sigma c$$

S = photoacoustic signal

C = Instrumental constant

P = (laser) power

α = Absorption coefficient

→ the intensity of the sound is proportional to the concentration of absorbing molecules

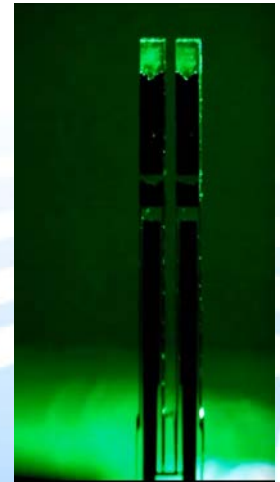
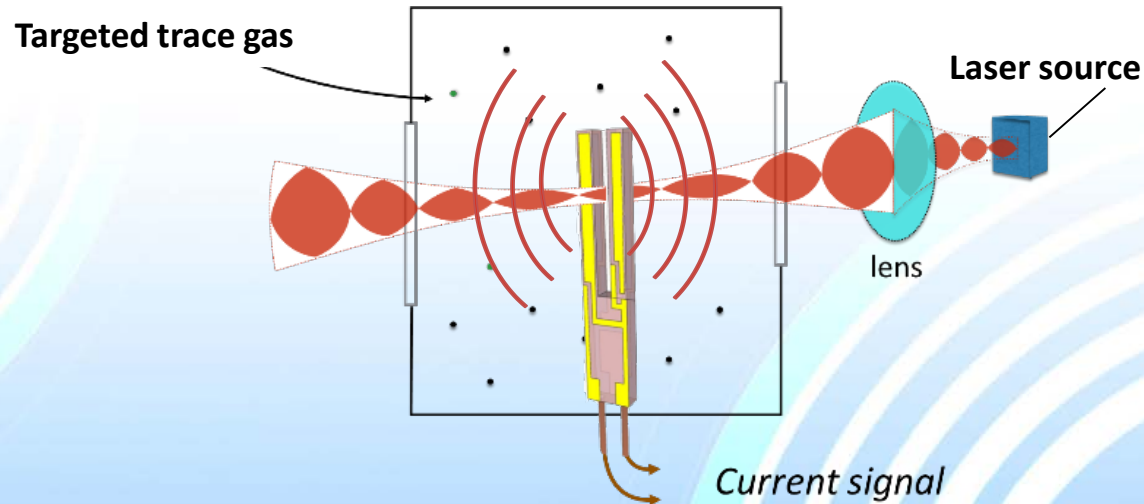
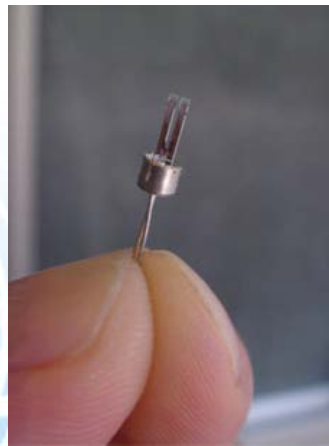
Why use the photoacoustic technique?

- Ⓢ Excellent sensitivity up to ppq with high power lasers
- Ⓢ Large dynamic range: linearity over a range of 10^6
- Ⓢ High resolution
- Ⓢ Fast measurements
- Ⓢ Capability of *in situ* detection
- Ⓢ Feasible costs, compact set-up, *coupled with semiconductor lasers*

Quartz-Enhanced Photoacoustic Spectroscopy

Introduction and Basic Operation

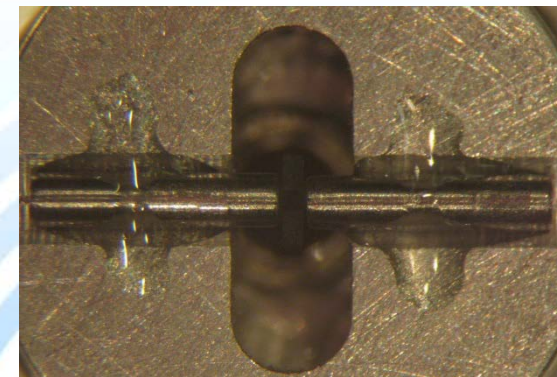
- Optical radiation is focused between the prongs of a quartz tuning fork
- Trace gases absorb optical energy at characteristic frequencies
- A pressure (sound) wave is generated by modulating the laser power
- Resonant mechanical vibration is excited by the sound waves
- The mechanical vibration is converted to an electrical signal via the piezoelectric effect
- The trace gas concentration is proportional to the electrical signal



Quartz-Enhanced Photoacoustic Spectroscopy

Merits and main characteristics

- Small sensing module and sample volume (a few cm^3)
- Wavelength independent
- ***Optical detector is not required***
- Wide dynamic range (from % to ppt)
- Immune to environmental acoustic noise
- Acoustic micro-resonator(s) to enhance the QEPAS signal



P. Patimisco, et al., Applied Physics Review,
B, Patimisco, 2018, Sensors 14, 6165, 2014
V. Spagnolo et al., Optics Letters, 37, 4461–4463, 2012

Quartz-Enhanced Photoacoustic Spectroscopy

Merits and main characteristics

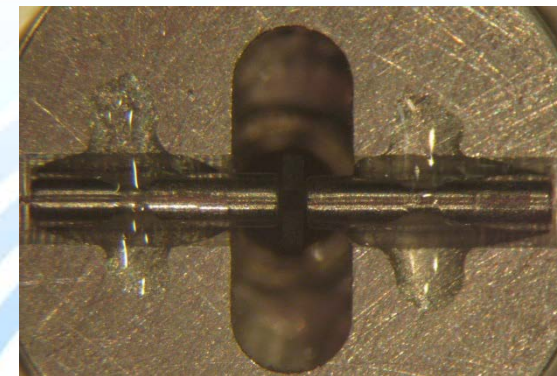
- Small sensing module and sample volume (a few cm³)
- Wavelength independent
- **Optical detector is not required**
- Wide dynamic range (from % to ppt)
- Immune to environmental acoustic noise
- Acoustic micro-resonator(s) to enhance the QEPAS signal



- Sensitivity scales with laser power
- Cross sensitivity issues
- Alignment (no light must hit the QTF or micro-resonators)
- Responsivity depends on the molecular energy transfer processes

Record sensitivity: 50 part-per-trillion

$\lambda = 10.54 \mu\text{m}$ (mid - IR), SF₆

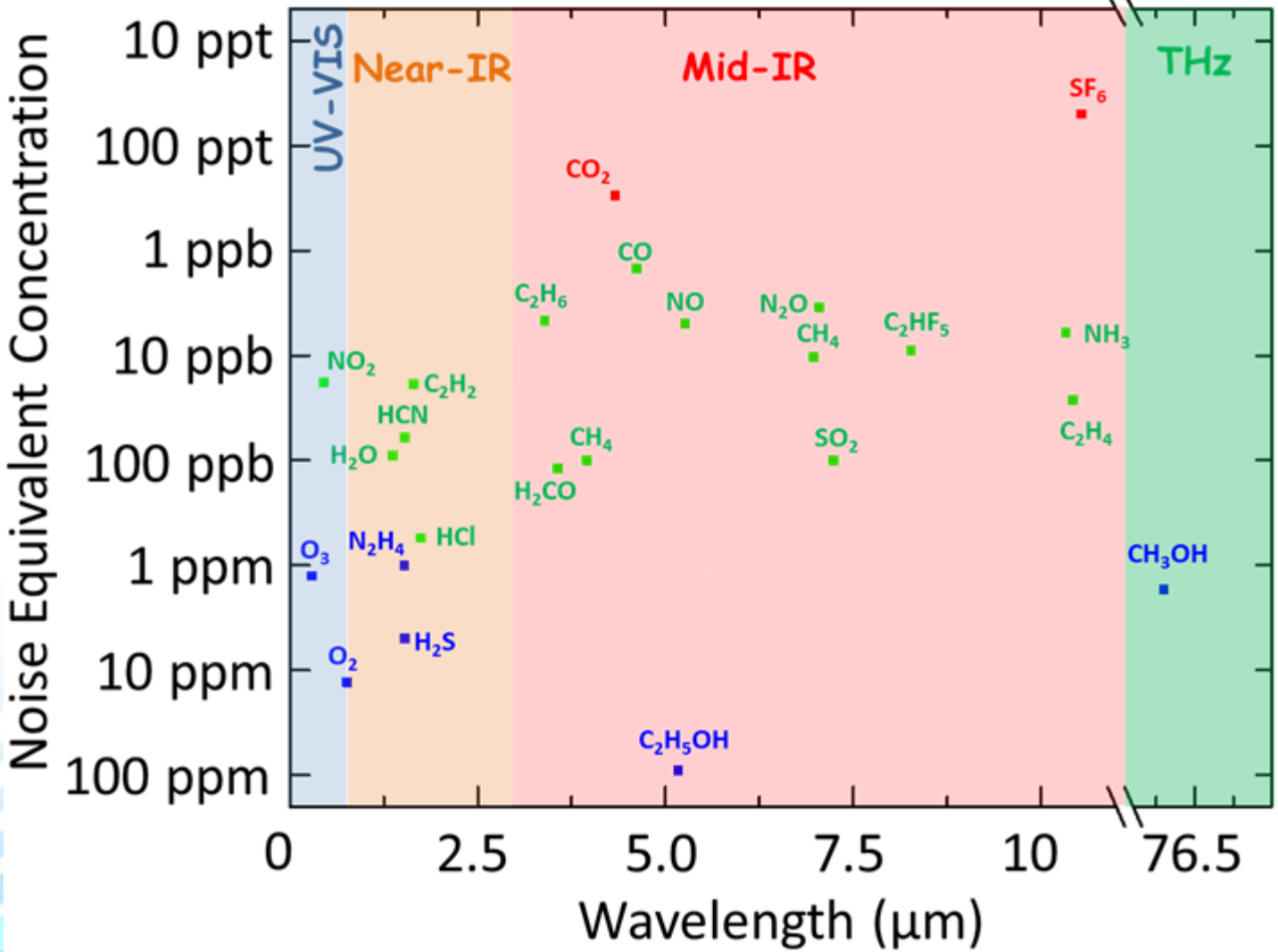


P. Patimisco, et al., Applied Physics Review,

5, 041106, 2018, Sensors 14, 6165, 2014

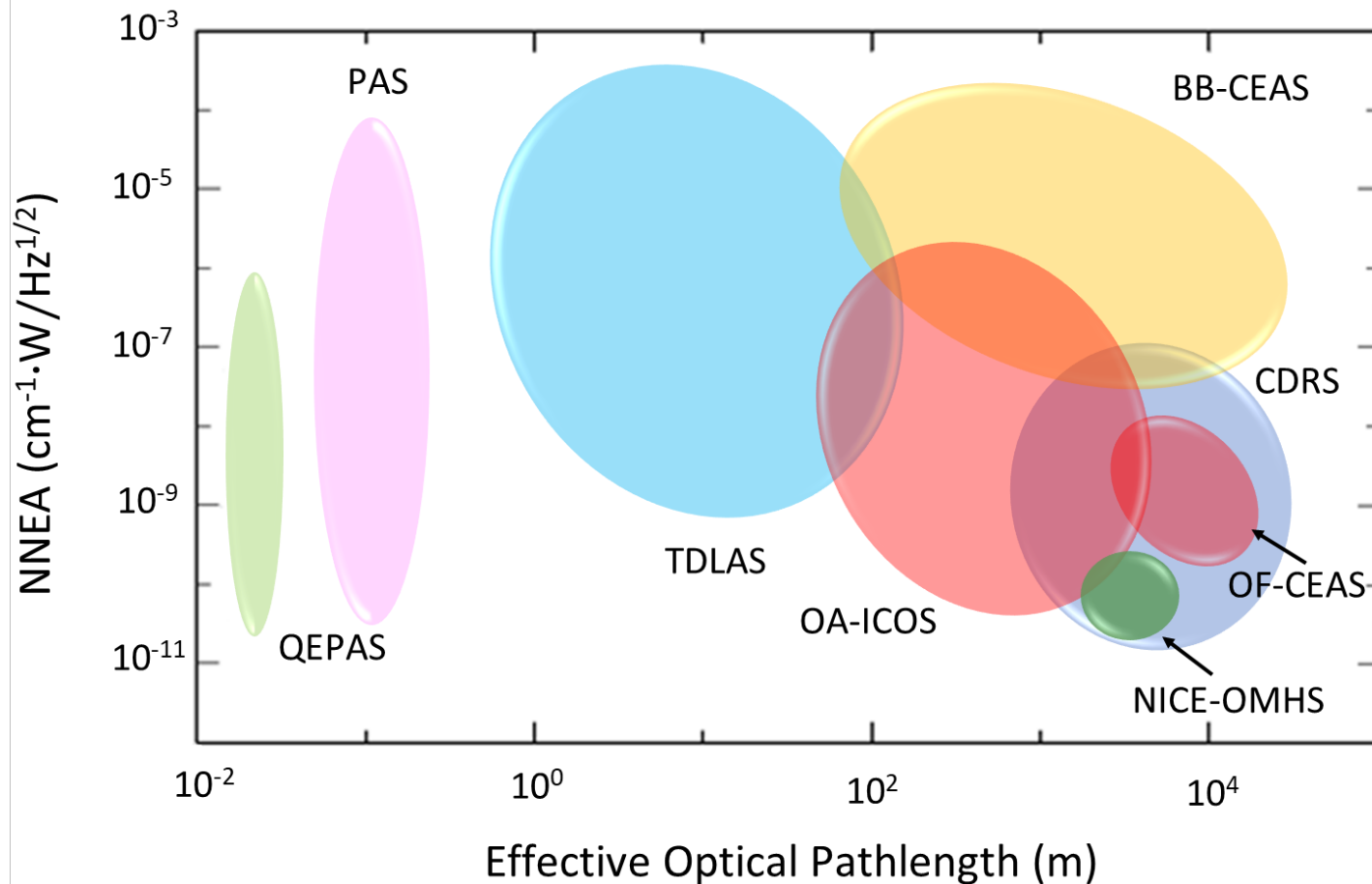
V. Spagnolo et al., Optics Letters, 37, 4461–4463, 2012

QEPAS gas sensing performance



Gas sensing techniques performances (Mid-IR)

P. Patimisco, G. Scamarcio, F.K. Tittel and V. Spagnolo, "Quartz-enhanced photoacoustic spectroscopy: a review", *Sensors*, 14, 6165-6206 (2014)



NNEA for categories of gas detection techniques as a function of optical path-length. Key: BB-CEAS—broadband cavity-enhanced spectroscopy, CRDS—cavity ring-down spectroscopy, OA-ICOS—off-axis integrated cavity output spectroscopy, OF-CEAS—optical feedback cavity-enhanced absorption spectroscopy, NICE-OMHS—noise-immune cavity-enhanced optical heterodyne spectroscopy, PAS photoacoustic spectroscopy, **QEPAS—Quartz-enhanced photoacoustic spectroscopy.**

OUTLINE

- Motivation for Gas Sensing
- Quartz Enhanced Photoacoustic Gas Detection
- QEPAS: Basic principles and merits
- **QEPAS with custom quartz tuning forks (2nd Generation)**
-

Quartz tuning fork

Gas absorption coefficient

QTF-dependent

Conversion efficiency: optical power \rightarrow sound

$$QEPAS\ Signal \propto P \cdot \alpha \cdot Q \cdot \epsilon$$

Laser power

QTF Q-factor

Euler-Bernoulli beam theory

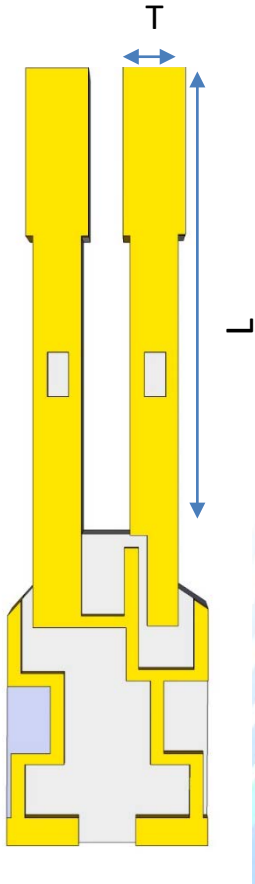
$$EI_y \frac{d^4 X}{dz^4} + \rho S \frac{d^2 X}{dt^2} = 0$$

Resonance Frequency, in-plane flexural modes

$$f_n = \frac{\pi T}{8\sqrt{12}L^2} \sqrt{\frac{E}{\rho}} n^2$$

$$n_{fund} = 1.19$$

$$n_{overt} = 3$$



Quartz tuning fork

Gas absorption coefficient

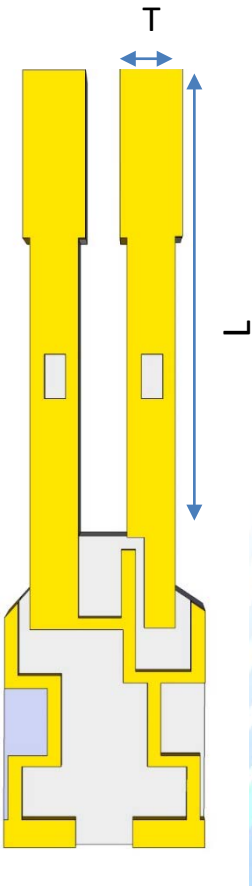
QTF-dependent

Conversion efficiency: optical power \rightarrow sound

$$QEPAS\ Signal \propto P \cdot \alpha \cdot Q \cdot \epsilon$$

Laser power

QTF Q-factor



Euler-Bernoulli beam theory

$$EI_y \frac{d^4 X}{dz^4} + \rho S \frac{d^2 X}{dt^2} = 0$$

Resonance Frequency, in-plane flexural modes

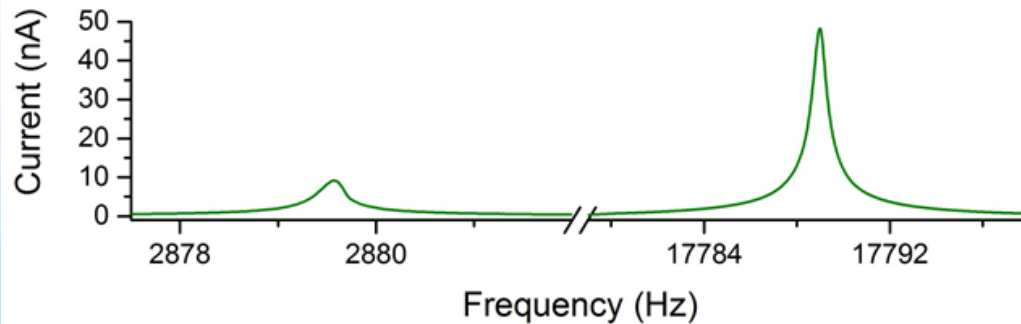


$$f_{1st\ overtone} \sim 6.2 \cdot f_{fundamental}$$

$$f_n = \frac{\pi T}{8\sqrt{12}L^2} \sqrt{\frac{E}{\rho}} n^2$$

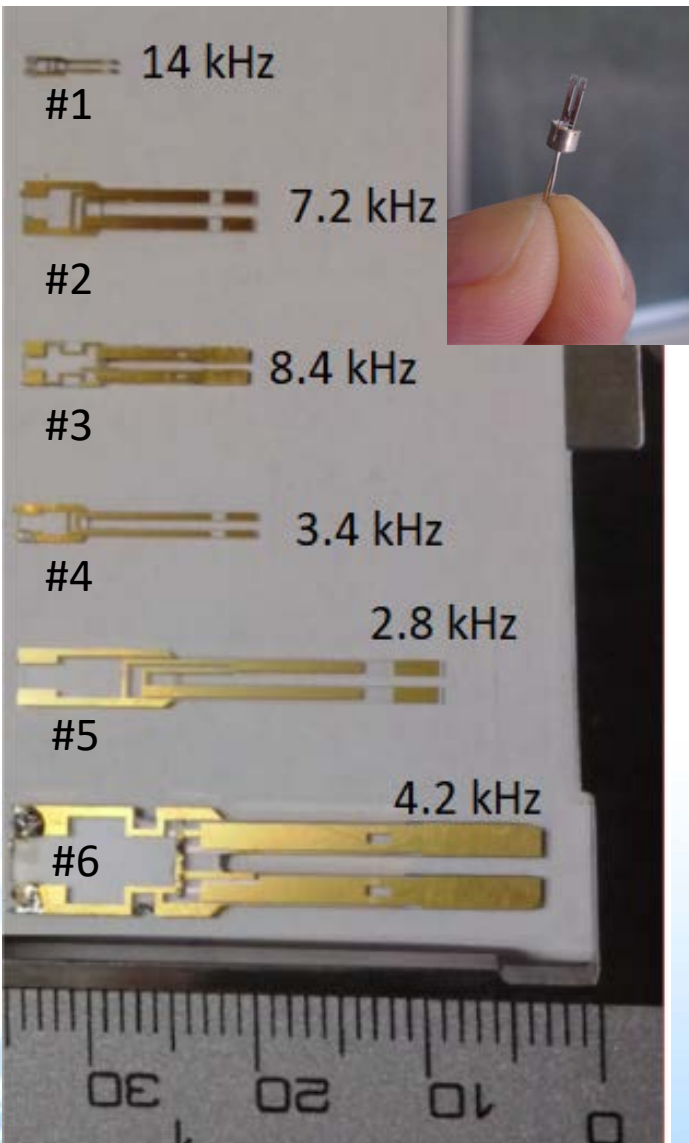
$$n_{fund} = 1.19$$

$$n_{overt} = 3$$

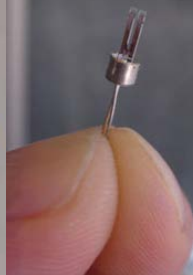
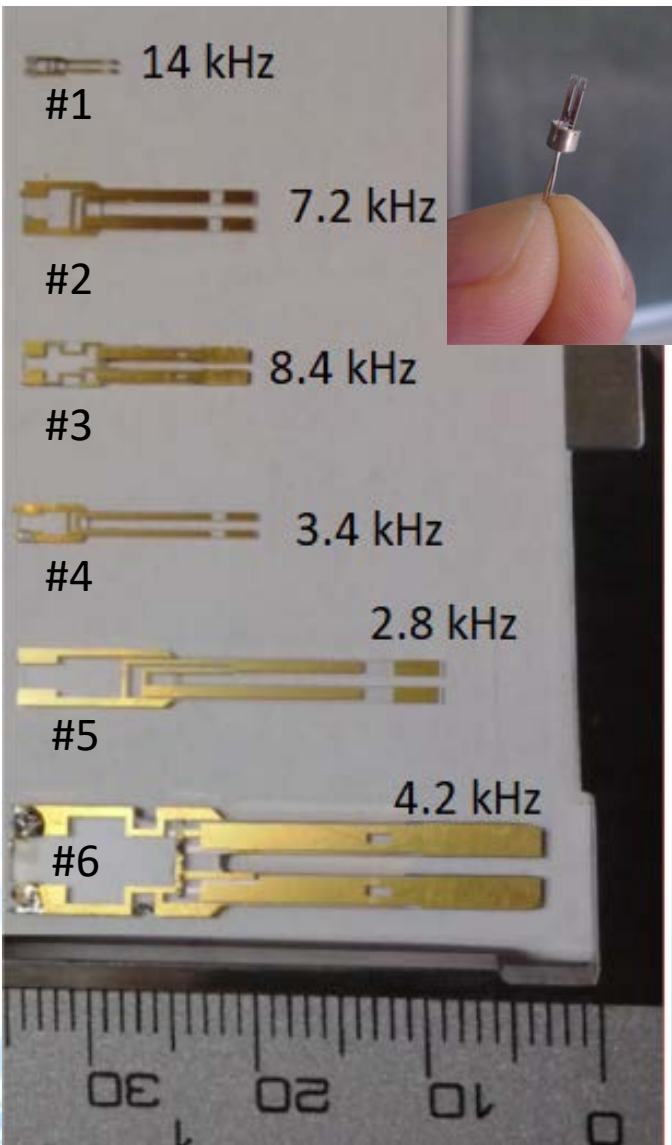


P. Patimisco, et al., *Analyst* 139, 2079, 2014.
 A. Sampaolo, et al., *Appl. Phys. Lett.*, 107, 231102, 2015.
 P. Patimisco et al., *Sens. Act, B Chem.* 227, 539, 2016.

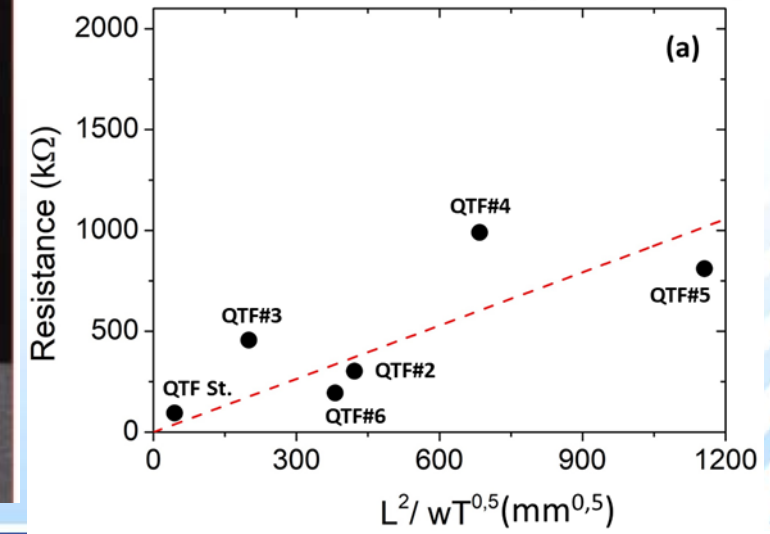
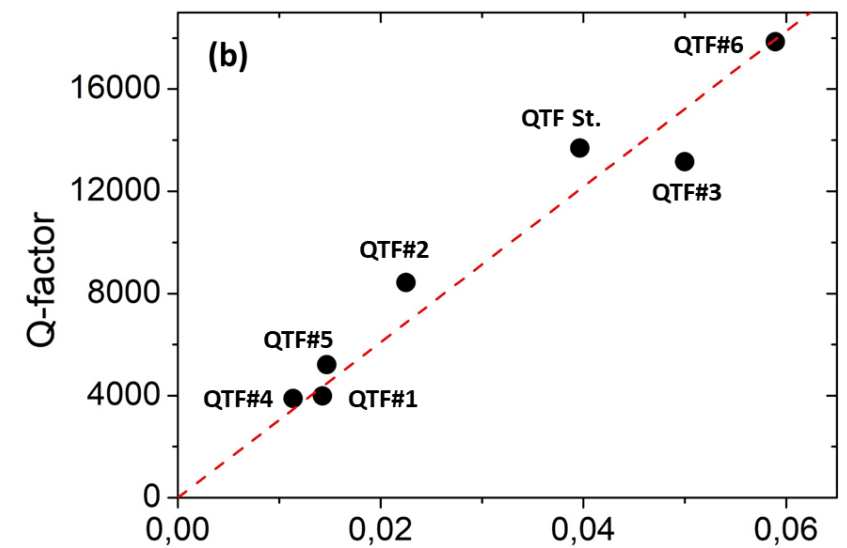
Custom QTF 2nd generation



Custom QTF 2nd generation



$$Q \propto wT/L$$

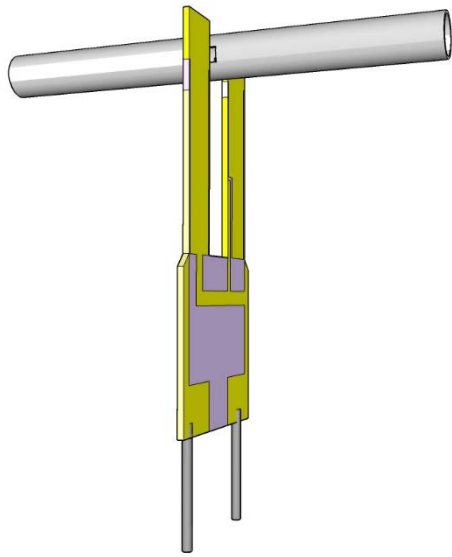


$$R \propto L^2/w\sqrt{T}$$

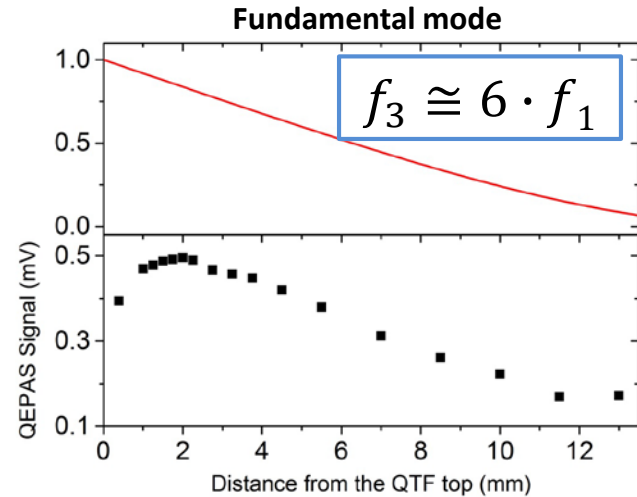
QTF DESIGN GUIDELINES

2nd generation main results

Single-tube microresonator



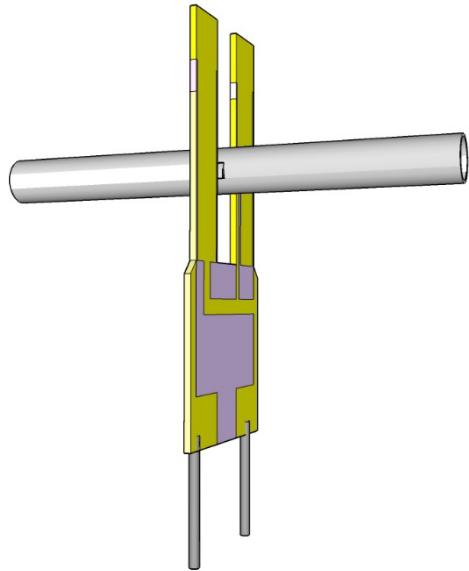
1st Overtone modes



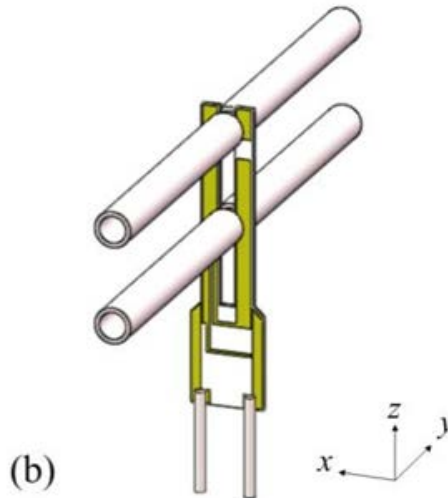
P. Patimisco, et al., Applied Physics Review, 5, 011106, 2017
H. Zengh, L. Dong, P. Patimisco et al, Applied Physics Letters, 110, 021101, 2017
L. Dong, P. Patimisco et al, Applied Physics Letters, 110, 021101, 2017
F. K. Tittel, A. Sampaolo, P. Patimisco et al., Optics

2nd generation main results

Single-tube microresonator

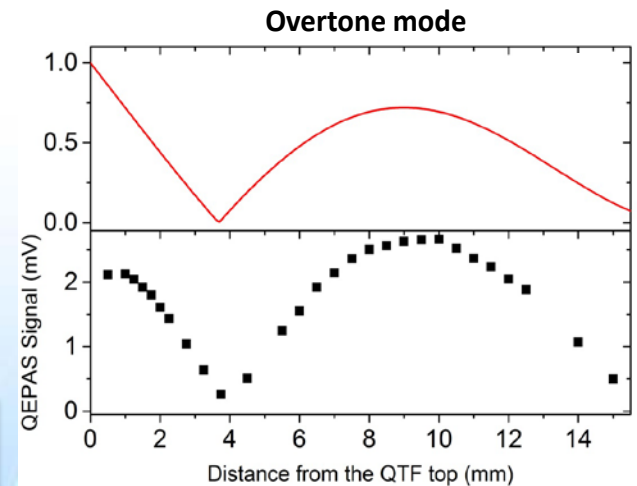
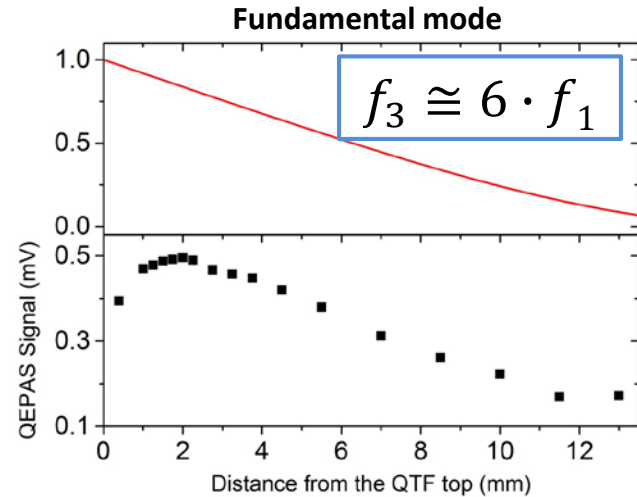


Double antinode excited SO-QEPAS



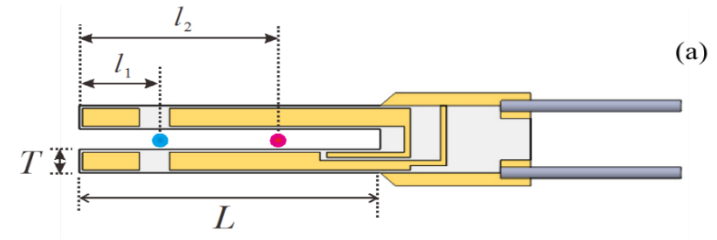
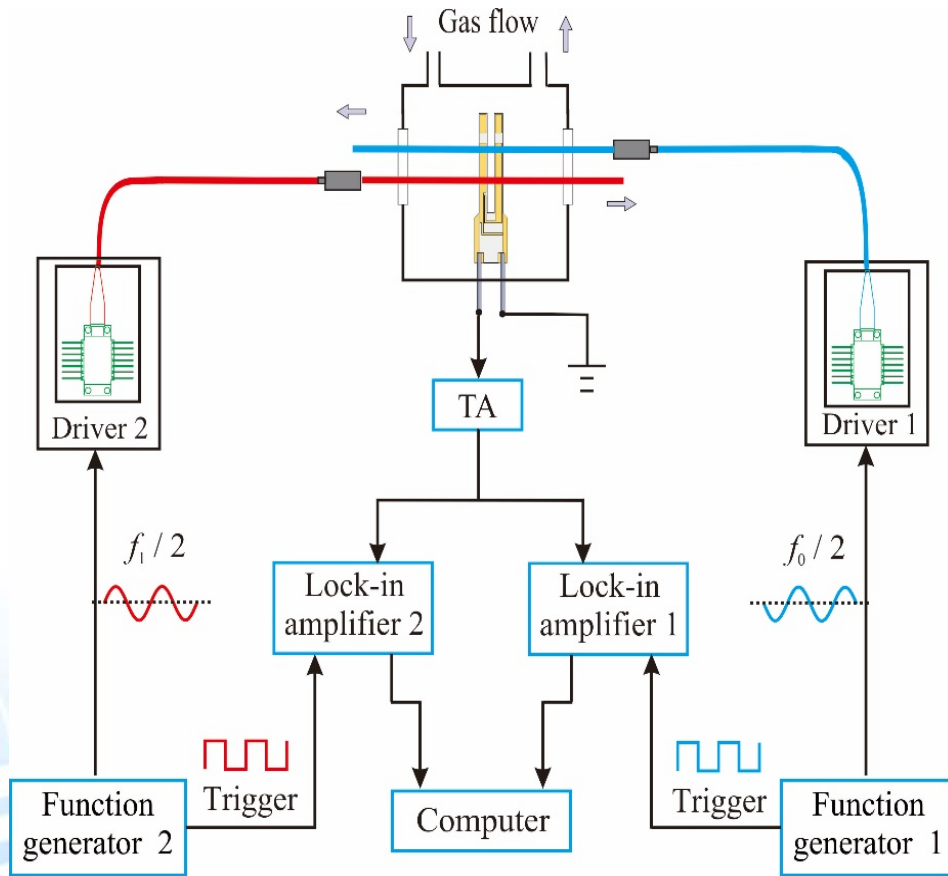
A SNR gain factor of **500** with respect to the bare QTF operating in the fundamental mode

1st Overtone modes



P. Patimisco, et al., Applied Physics Review, 5, 011106, 2017
 H. Zengh, L. Dong, P. Patimisco et al, Applied Physics Letters, 110, 021101, 2017
 H. Zengh, L. Dong, P. Patimisco et al, Applied Physics Letters, 110, 021101, 2017
 F. K. Tittel, A. Sampao, P. Patimisco et al., Optics

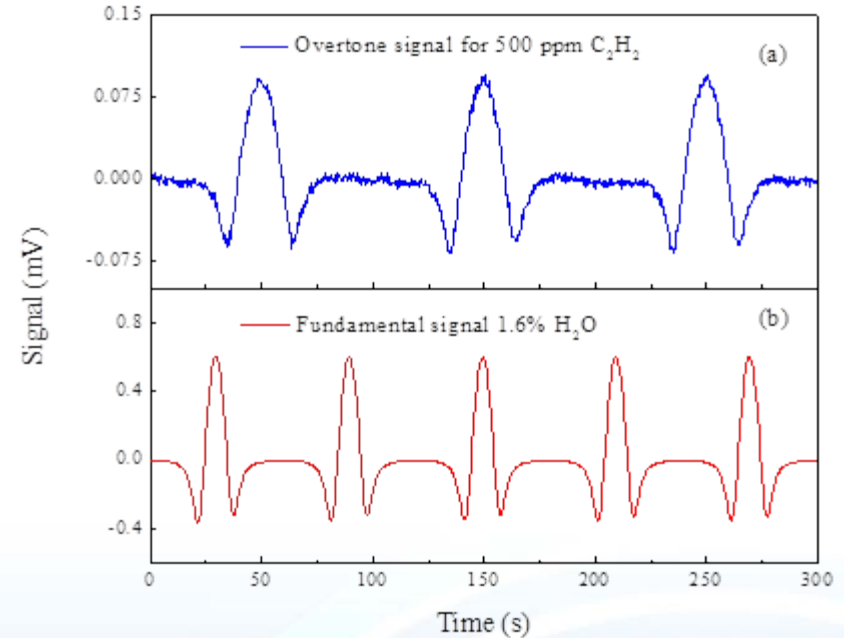
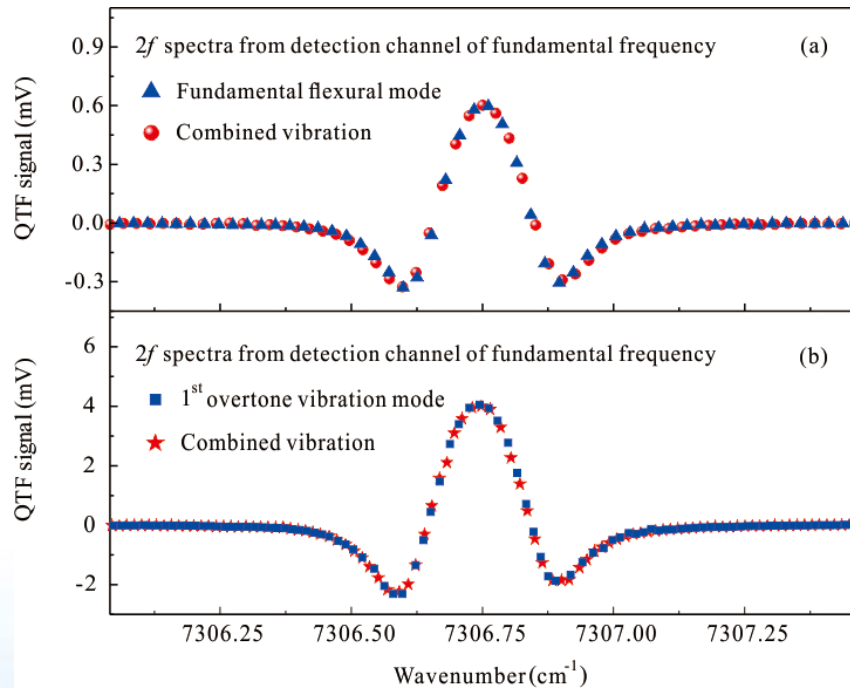
Dual-gas QEPAS operating at both the QTF fundamental and 1st overtone



Two beams from two independently modulated lasers are focused between the prongs of a quartz tuning fork at two different positions to excite both the fundamental and first overtone flexural modes simultaneously

Dual-gas quartz-enhanced photoacoustic spectroscopy (QEPAS) sensor system based on a frequency division multiplexing technique

Dual-gas QEPAS operating at both the QTF fundamental and 1st overtone



- No cross-talk between fundamental and 1st overtone
- Simultaneously dual-gas detection (eg. C₂H₂ and H₂O)
- Future improvements using single-tube resonators
- Applications include: industrial process control, isotope ratio measurements, breath analysis

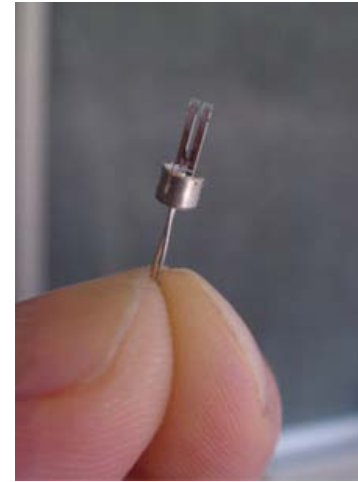
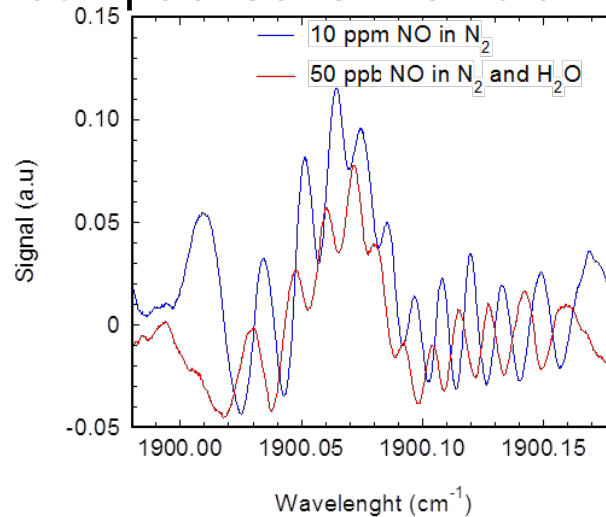
OUTLINE

- Motivation for Gas Sensing
- Quartz Enhanced Photoacoustic Gas Detection
- QEPAS: Basic principles and merits
- QEPAS with custom quartz tuning forks
- **QEPAS in the THZ range**
-

QEPAS sensors in the THz range

Standard QTFs are characterized by a compact sensitive volume ($\sim 0.3 \times 0.3 \times 3 \text{ mm}^3$)

In QEPAS experiments, it is critical to avoid laser illumination of the QTF, since the radiation blocked by the QTF prongs, generates an undesirable non-zero background which carries a shifting fringe-like interference pattern.



The limited space ($300 \mu\text{m}$) between the QTF prongs is comparable with the wavelength of THz sources so far has represented the main limitation for the use in QEPAS-based sensor systems in the THz range.

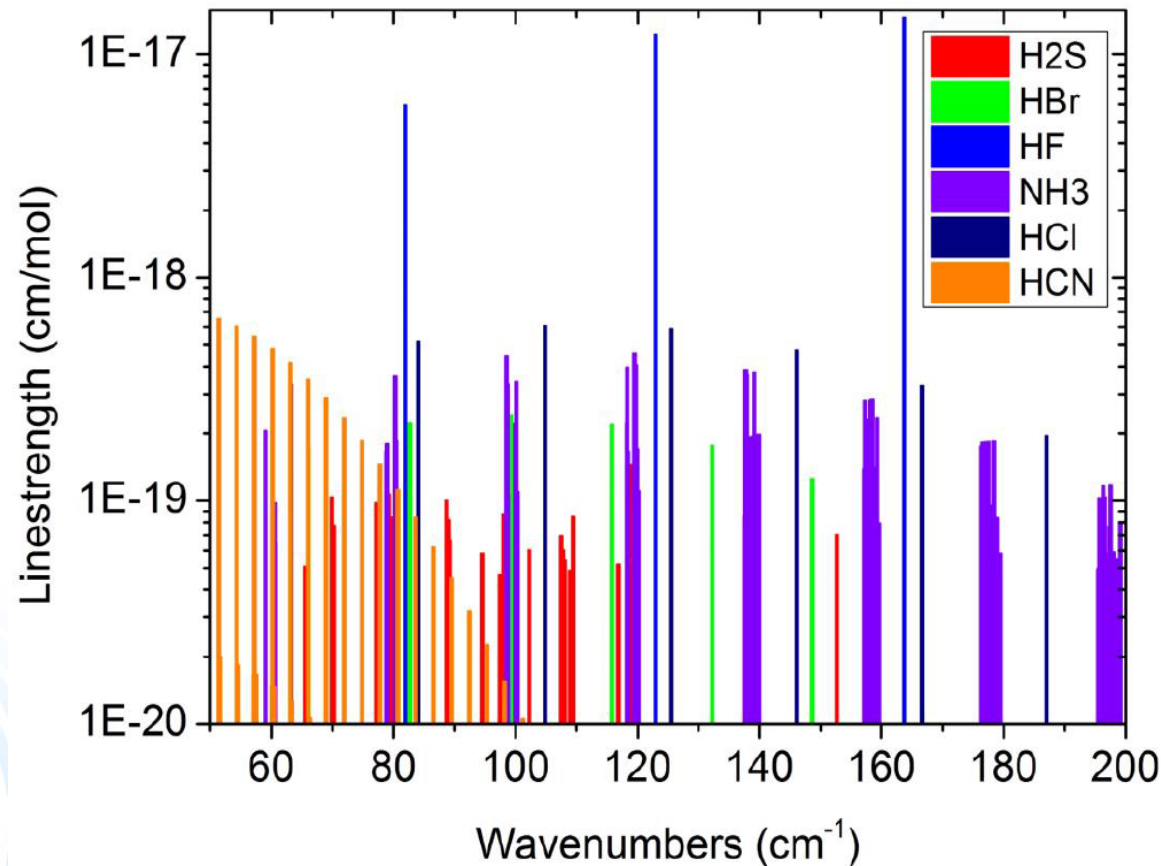
Larger sized QTFs are mandatory to operate in the THz

S. Borri et al., Applied Physics Letters, 103, 021105, **2013**

P. Patimisco et al., Analyst, 139, 2079-2087, **2014**

P. Patimisco et al., "QEPAS Review", Sensors, 14, 6165–6206, **2014**.

Why THz QEPAS Spectroscopy?



Several gas species such as HF, OH, HCN, HCl, HBr, NH₃, H₂O₂, H₂S, H₂O, explosive (vapour phase) etc. show strong absorption bands in the THz spectral range.



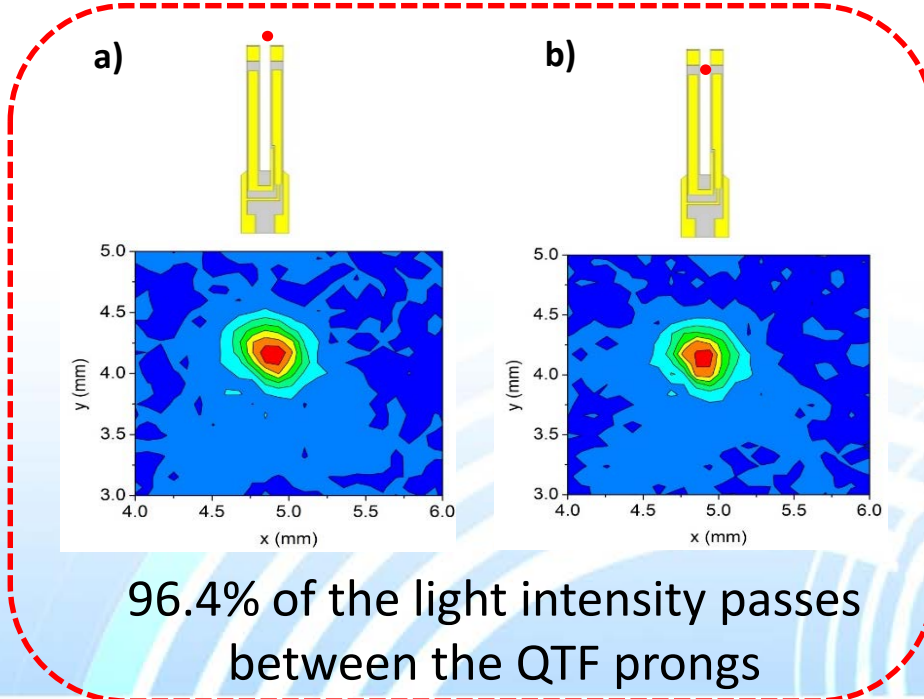
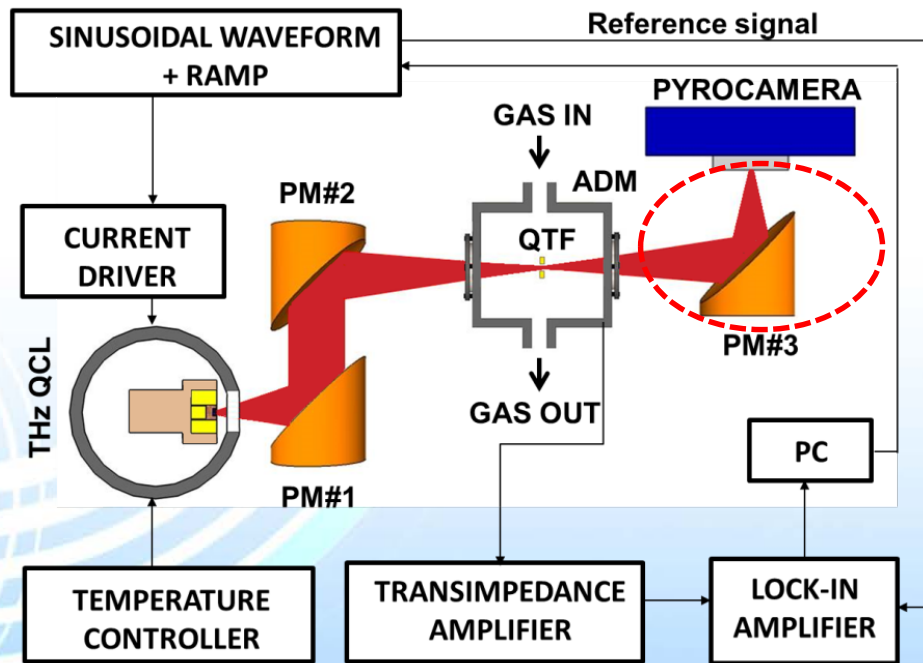
Mainly rotational levels are involved in THz absorption processes and rotational-translational (R-T) relaxation rates are **up to three order of magnitude faster** with respect to vibrational-translational (V-T).

THz QEPAS results employing a Novel Custom QTF



Methanol (CH_3OH)
detection

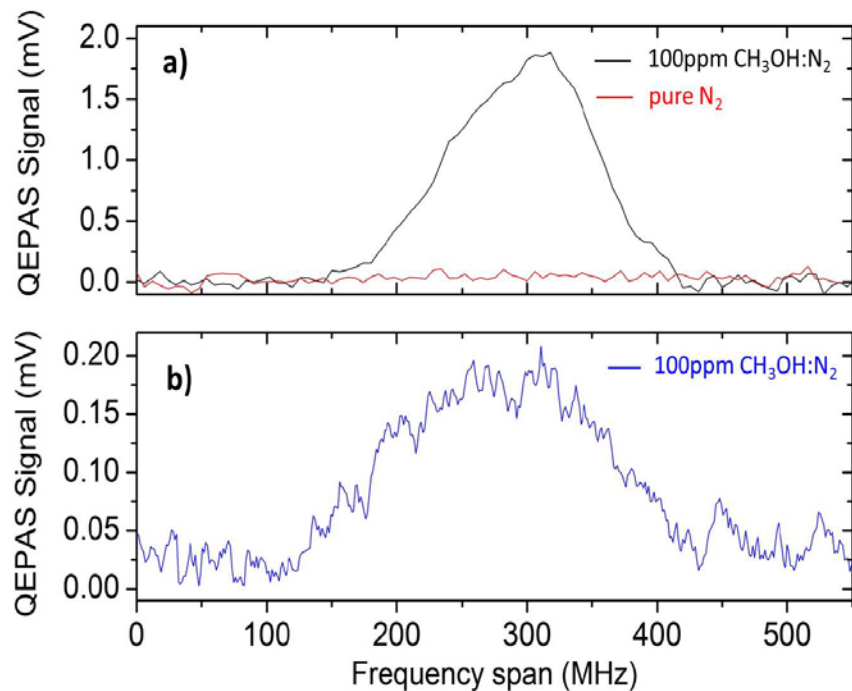
- Wavenumber: 131.054 cm^{-1} (3.93 THz)
- Absorption line-strength: $4.28 \times 10^{-21} \text{ cm/mol}$
- Optical power: $40 \mu\text{W}$



96.4% of the light intensity passes between the QTF prongs

THz QEPAS results employing a Novel Custom QTF

100 ppm of methanol in N₂ at P=10 Torr

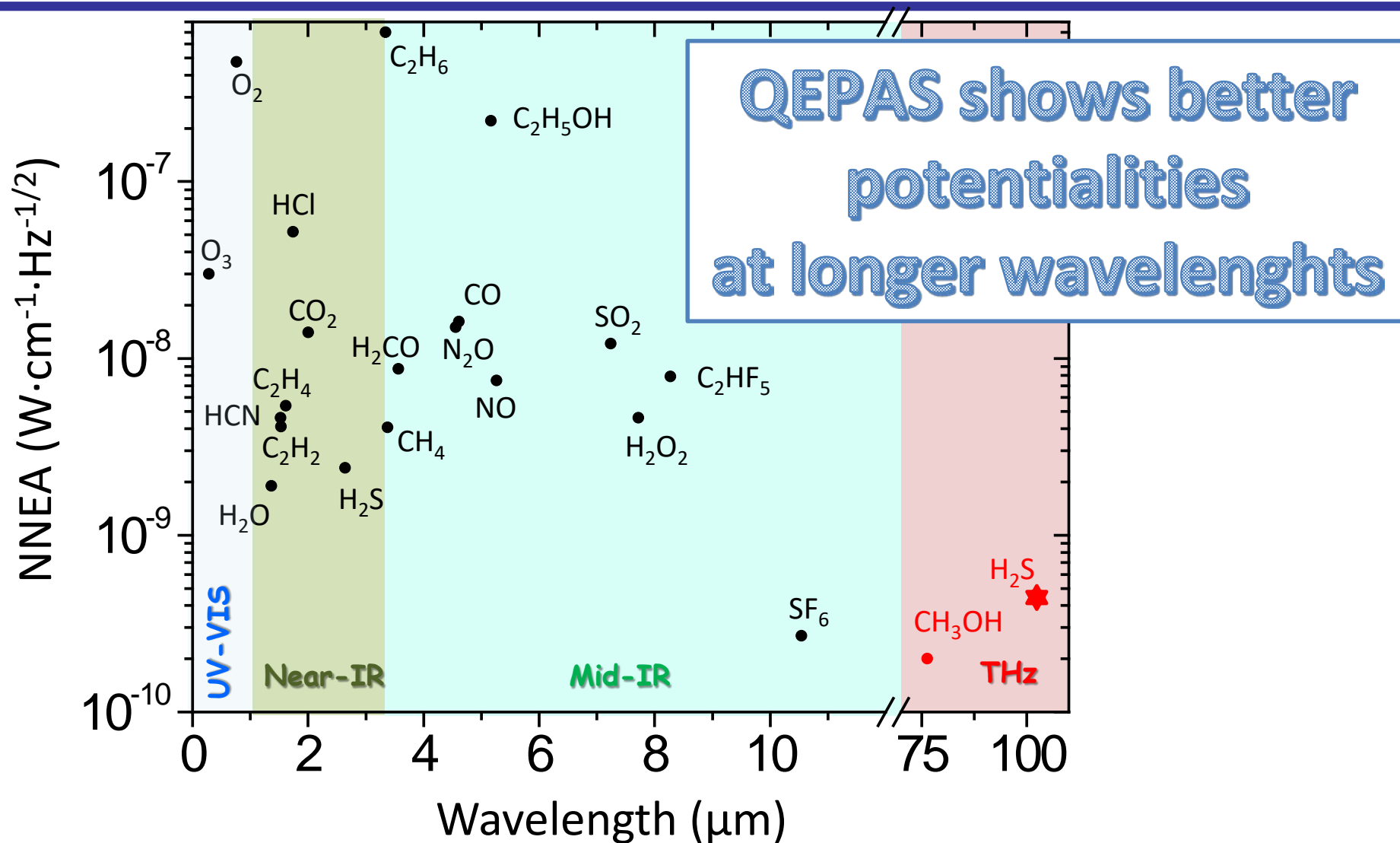


Comparison between QTFs with custom and new geometry

- Same noise level
- Signal to noise ratio (SNR) and Sensitivity 9x better for QEPAS system employing a QTF with new geometry
- @ 30 sec integration time: Sensitivity = 160ppb and
- NNEA = $3.75 \times 10^{-11} \text{ cm}^{-1} \text{ W/vHz}$

QEPAS RECORD

QEPAS Performance for Trace Gas Species: NNEA vs λ



Fast energy relaxation rates of THz rotational transition allows to **operate at low pressure**, so taking advantages of the **very high QTF Q-factors** and enhanced selectivity.

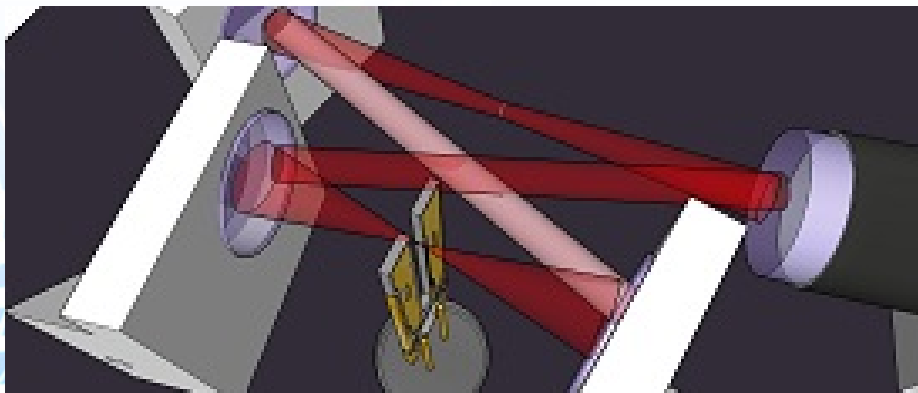
Intracavity QEPAS

Basics

Three main criteria drive the development of high-sensitivity optical sensors:

- i) Selection of optimal molecular transition in terms of absorption strength
- ii) Long optical absorption length and/or use of buildup optical cavity;
- iii) Efficient spectroscopic detection schemes, e.g. photoacoustic spectroscopy (PAS)

QEPAS sensitivity scale with optical power



Cavity-Enhanced Absorption

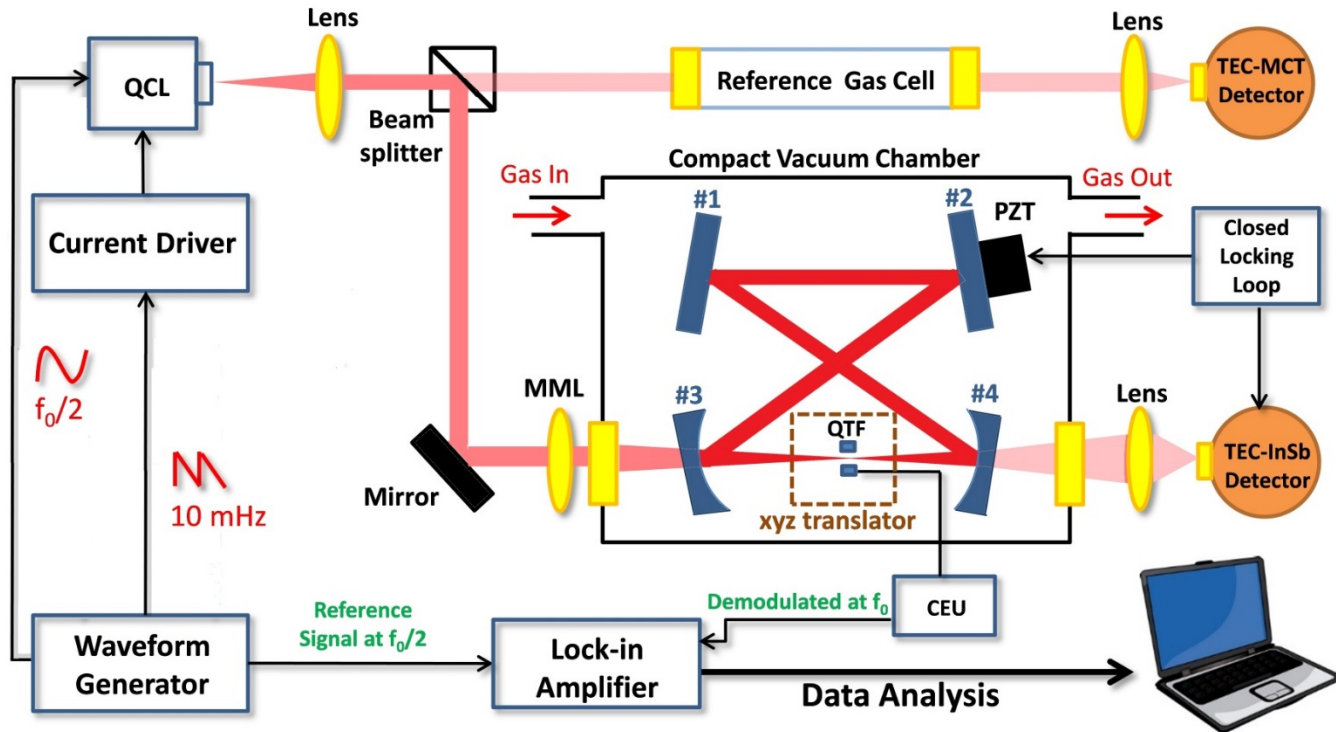


QEPAS



Intra-cavity QEPAS

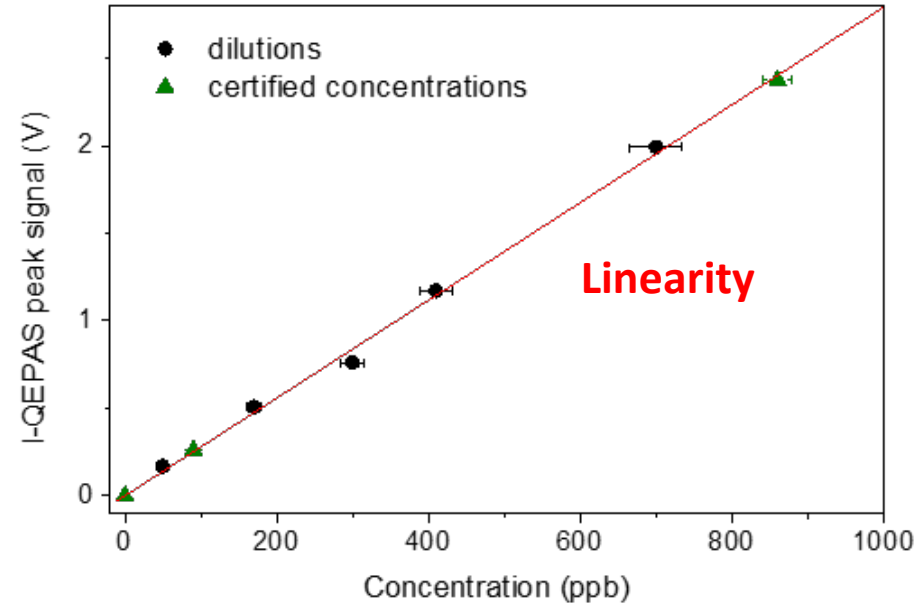
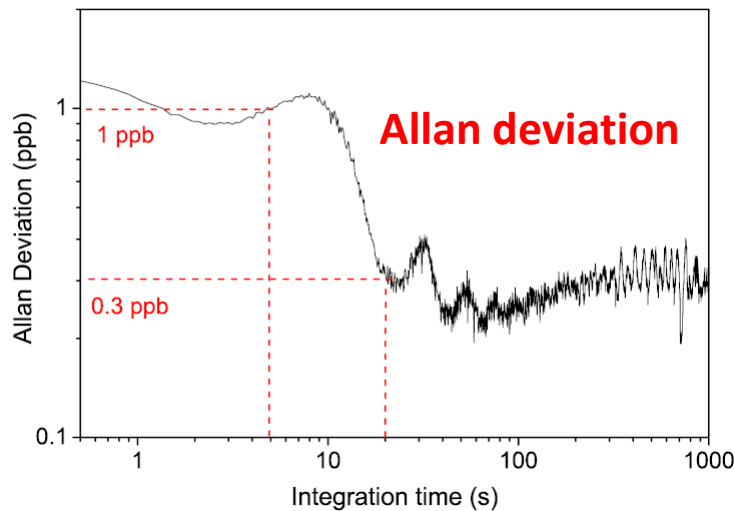
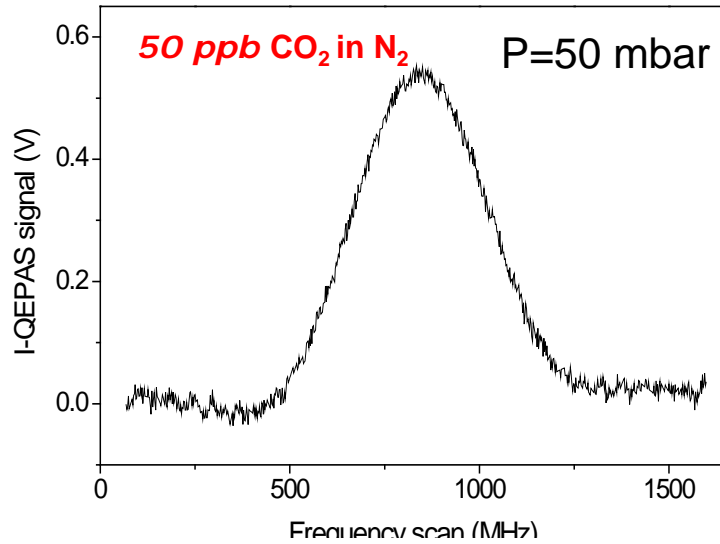
Intracavity-QEPAS setup



- RT CW DFB **Q**uantum **C**ascade **L**aser $\lambda = 4.33 \mu\text{m}$ ($P = 3\text{mW}$)
- Home-made low-noise current driver \rightarrow **laser linewidth** $\sim 1 \text{ MHz}$
- **Bow-tie cavity** \rightarrow 4 high reflectivity mirrors, $R = 99.9\%$
- **Electronic control-loop** + **PZT motor** lock cavity resonant frequency to the laser one

Intracavity optical power enhancement factor = 240

Performance and long term stability



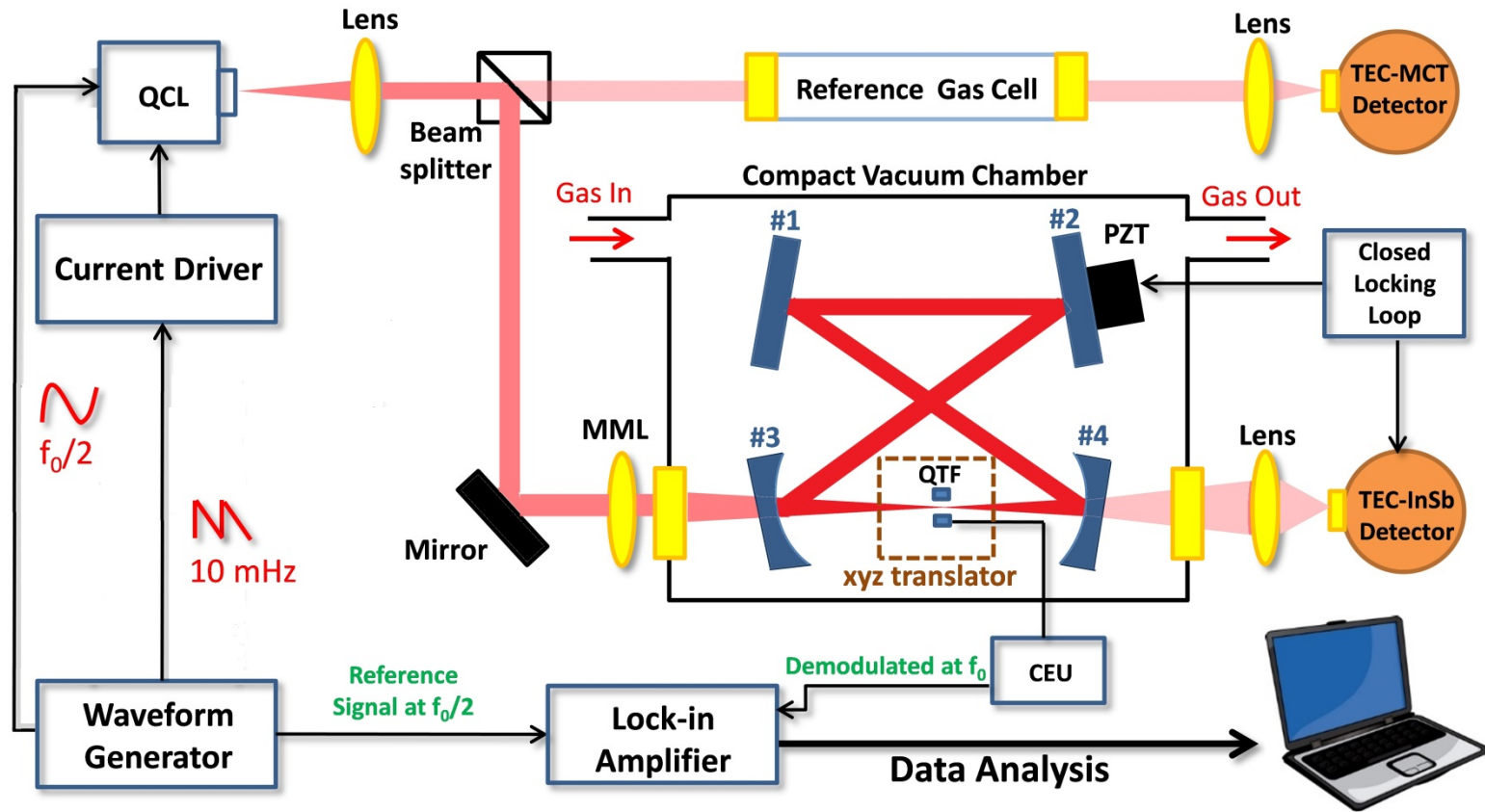
Noise Equivalent Concentration:

NEC = **300 ppt** @ 20sec integration time
(4sec lock-in time constant)

Absorption Coefficient Normalized to
detection bandwidth and optical power:

$$\text{NNEA} = \mathbf{3.2 \times 10^{-10} \text{ cm}^{-1} \text{ W}(\text{Hz})^{-1/2}}$$

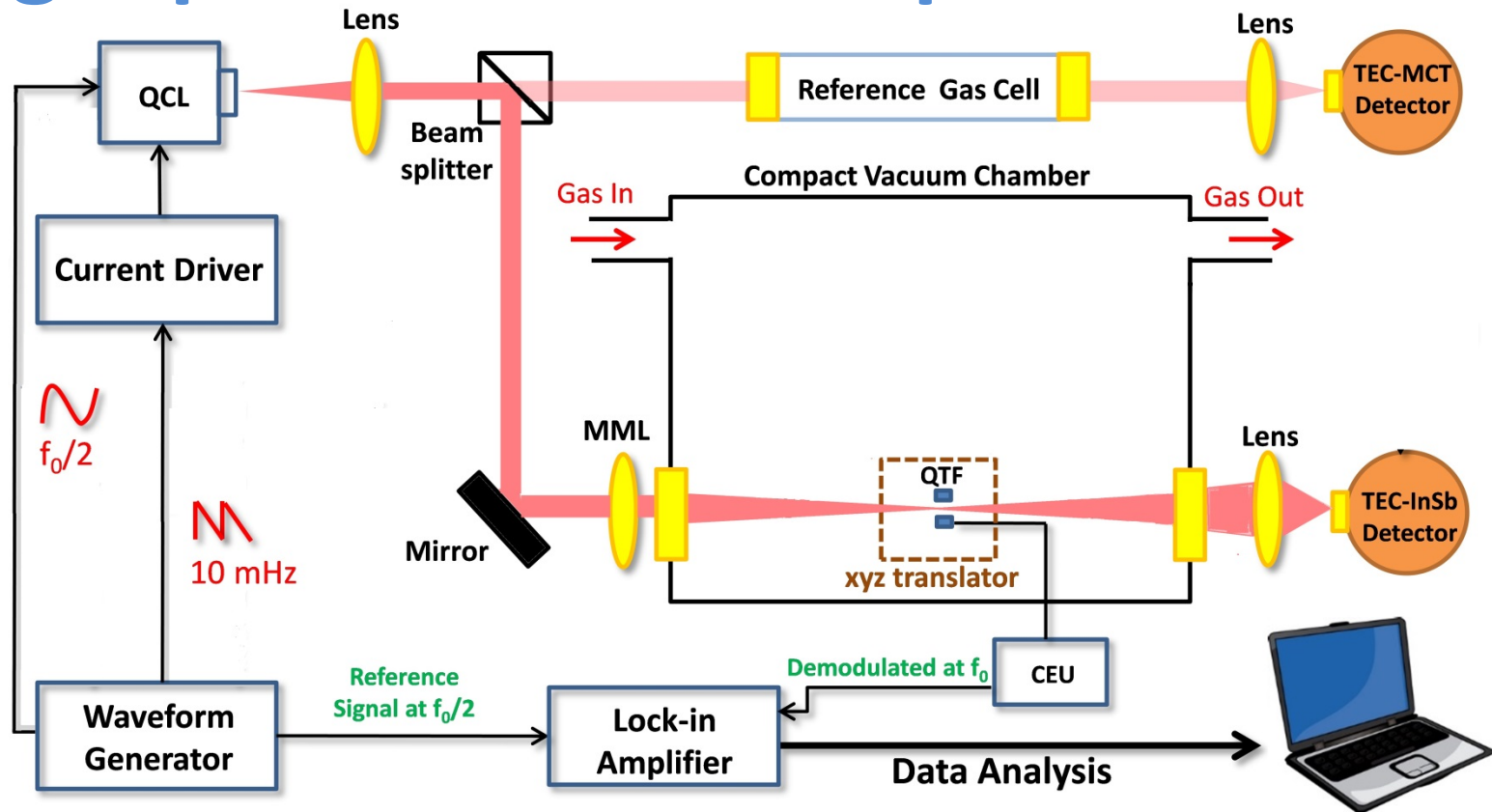
“Single-pass” QEPAS setup



Optical power build-up cavity removed

- Same optical power 3 mW
- Same gas pressure in the chamber 50 mbar
- Wavelength modulation approach and f_0 detection

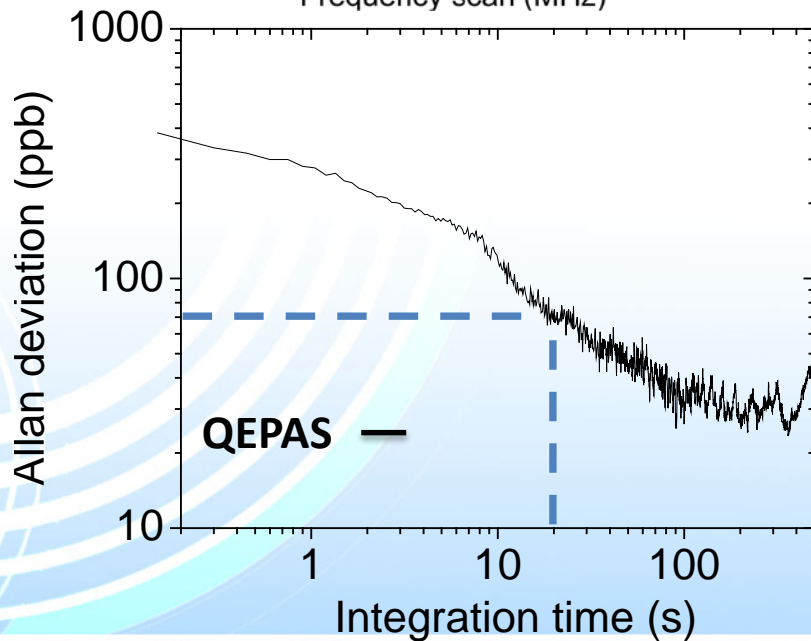
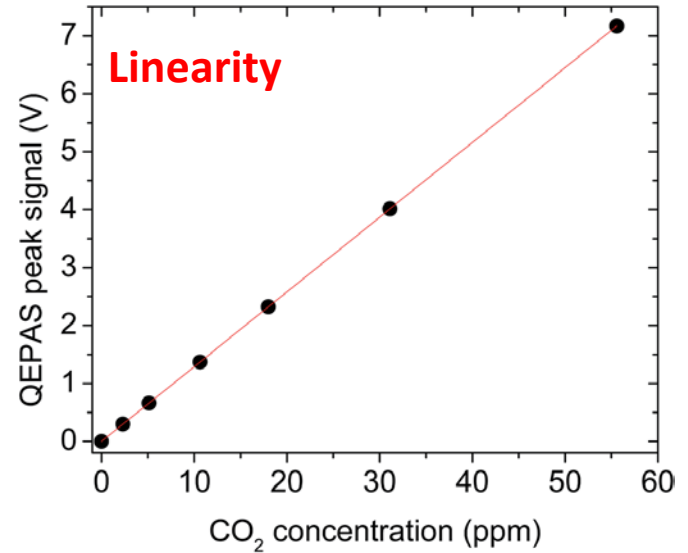
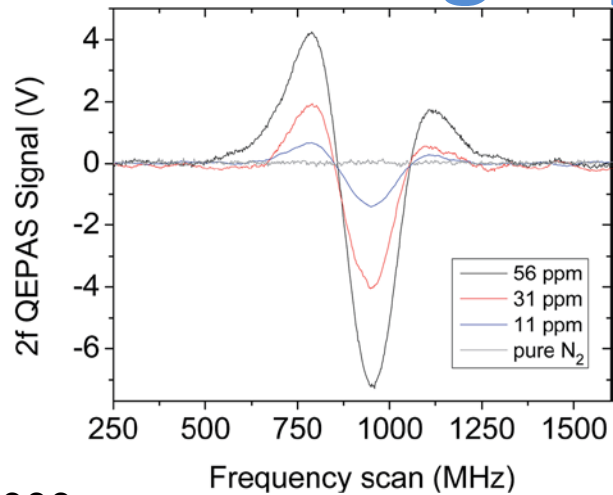
“Single-pass” QEPAS setup



Optical power build-up cavity removed

- Same optical power 3 mW
- Same gas pressure in the chamber 50 mbar
- Wavelength modulation approach and f_0 detection

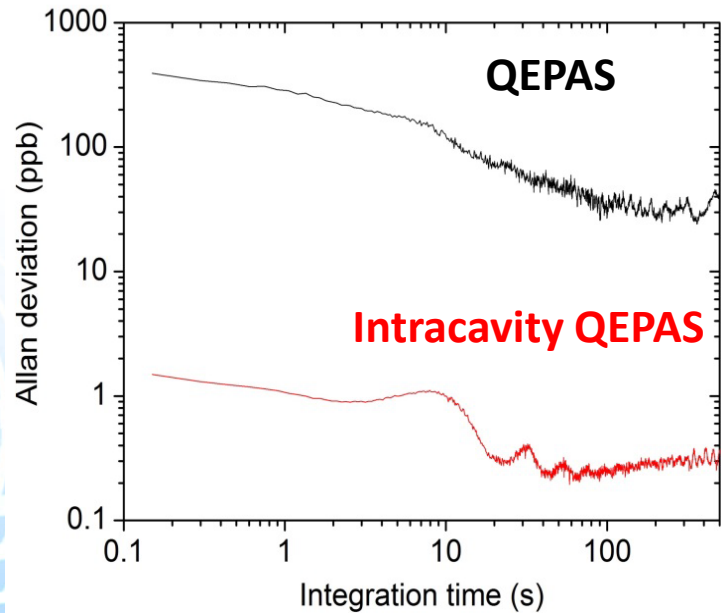
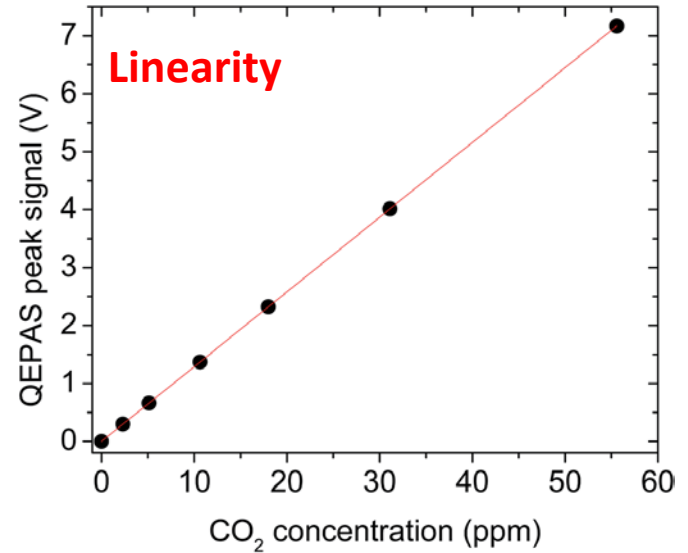
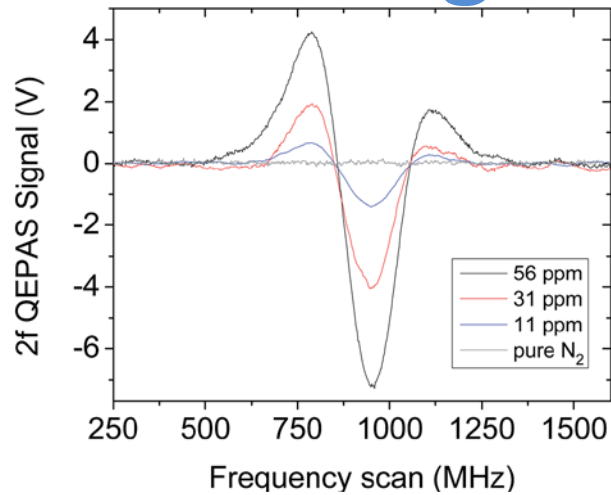
Standard single-pass QEPAS performances



NEC = **70 ppb** @ 20sec integration time

NNEA = **$7,5 \times 10^{-8} \text{ cm}^{-1} \text{ W}(\text{Hz})^{-1/2}$**

Standard single-pass QEPAS performances



NEC = **72 ppb @ 20sec** integration time

$$\text{NNEA} = 7,5 \times 10^{-8} \text{ cm}^{-1} \text{ W}(\text{Hz})^{-1/2}$$

A factor **234** bigger than **I-QEPAS**

Comparable with intracavity enhancement : 240

OUTLINE

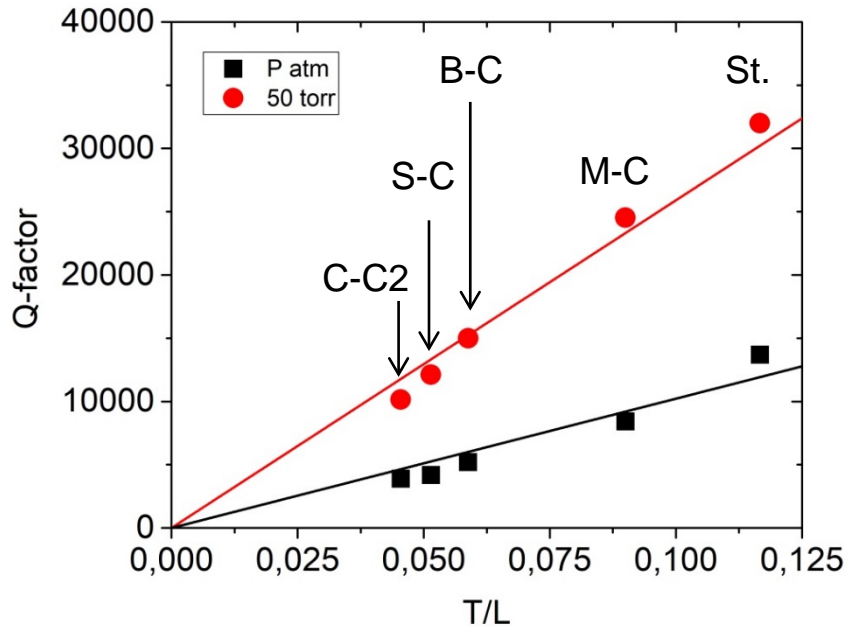
- Motivation for Gas Sensing
- Quartz Enhanced Photoacoustic Gas Detection
- QEPAS: Basic principles and merits
- **QEPAS with custom quartz tuning forks (3rd Generation)**

•

3rd generation of custom QTFs

Objective: Design of QTFs with a **high Q-factor** and resonant frequency in the range 15-17 kHz

Starting from QTFs 2nd generation



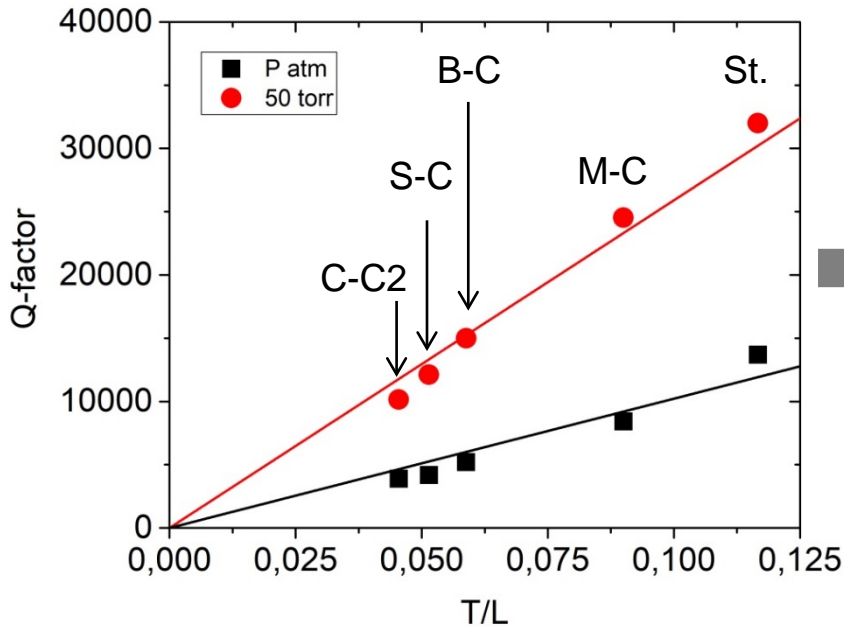
Air damping
dominates

$$Q \propto \frac{T}{L}$$

3rd generation of custom QTFs

Objective: Design of QTFs with a **high Q-factor** and resonant frequency in the range 15-17 kHz

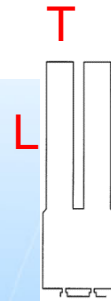
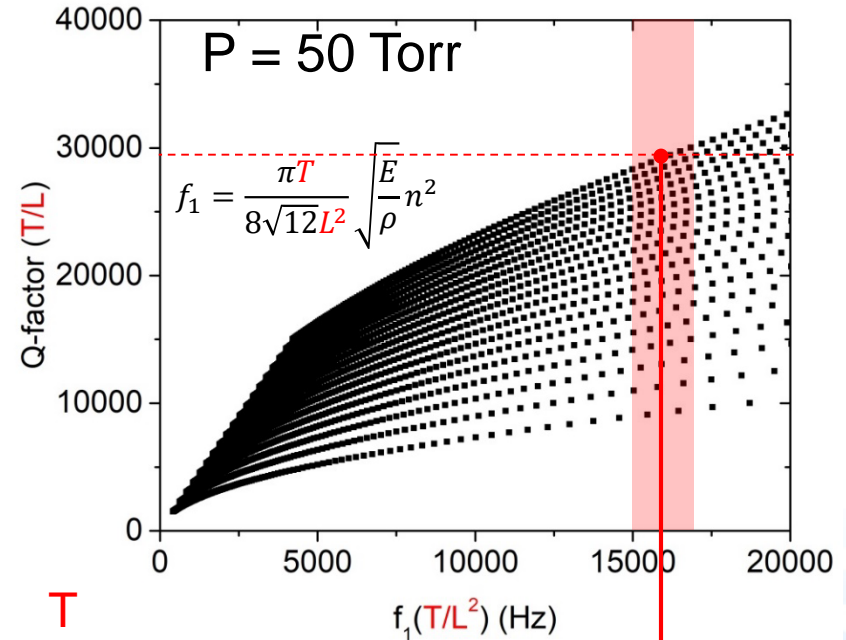
Starting from QTFs 2nd generation



Air damping dominates

$$Q \propto \frac{T}{L}$$

Simulation



Selected design:

$L = 9.4 \text{ mm}$

$T = 2 \text{ mm}$

$Q \sim 30000 \text{ @ } 50 \text{ Torr}$

$Q \sim 10000 \text{ @ } \text{Atm P.}$

3rd generation of custom QTFs

Goal: Realize custom quartz tuning forks, targeting: i) reduction of the resonance frequency; 2) maintenance of a high the Q-factor; 3) optimized electrode layout for overtone flexural mode

5 NEW DESIGNS



QTF S08

(prongs spacing 0.8 mm)

Reducing air damping while keeping f_0 15-17 kHz



QTF S08 - G

(prongs spacing 0.8 mm)

Grooves engraved on both sides of the QTF prongs



QTF S08 - TOP

(prongs spacing 0.8 mm)

Wider top end on both prongs



QTF S15

(prongs spacing 1.5 mm)

Increased prong spacing of 1.5 mm to facilitate optical alignment of the focused laser beam



QTF-Overtone

(prongs spacing 0.7 mm)

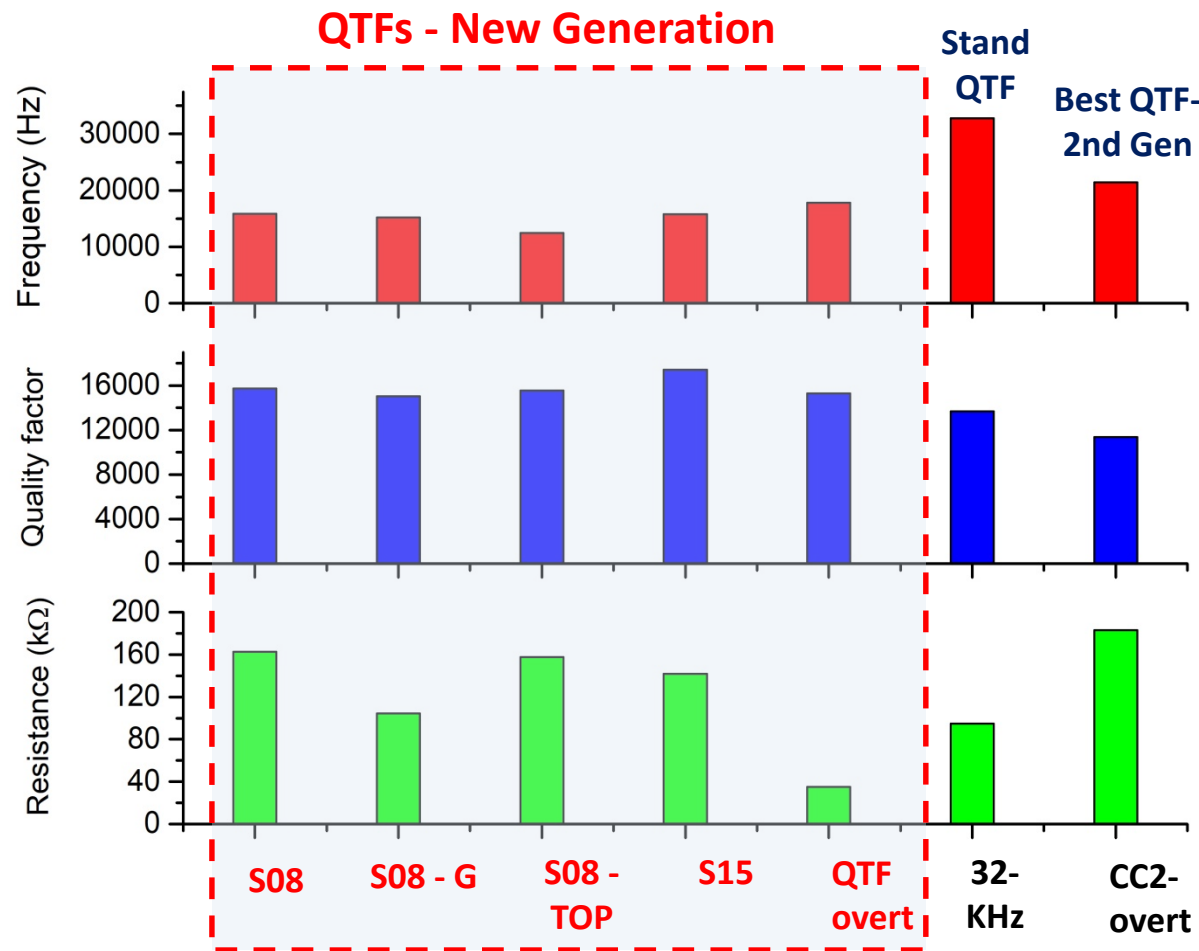
Enhanced overtone mode operation @ 17 kHz with an optimized electrode layout design

All these QTFs have the same prong length and thickness

P. Patimisco et al, Optics Letters 43, 1854-1857, 2018

P. Patimisco et al, IEEE T. Ultr. Ferr. 65, 1951-1957,

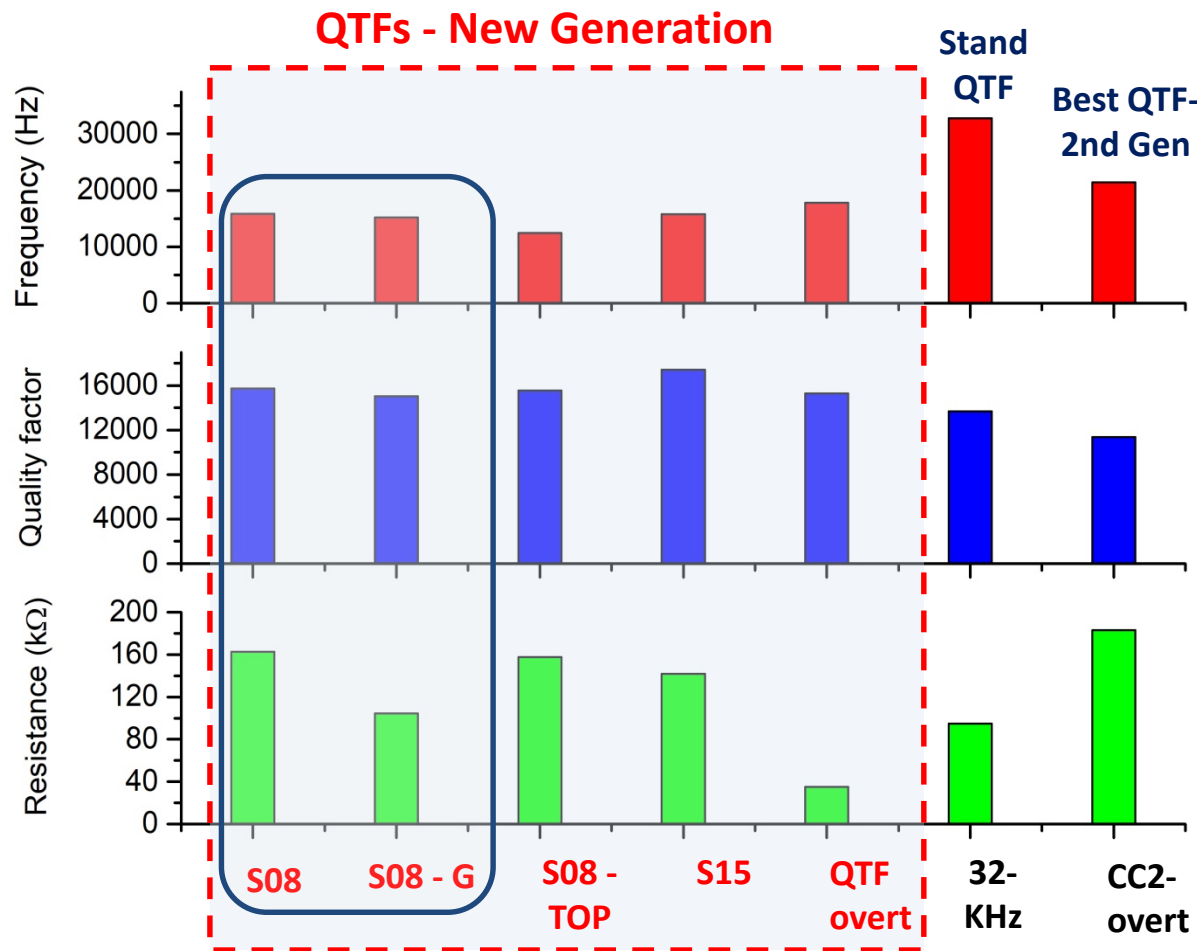
3rd gen. QTFs Electrical Characterization



Results are compared with a *standard 32 kHz-QTF* and the *best QTF of the 2nd generation (C-C2, overtone)*

- The **frequency was decreased by a factor of 2** with respect to the 32 KHz-QTF achieving **higher quality Q-factors**.

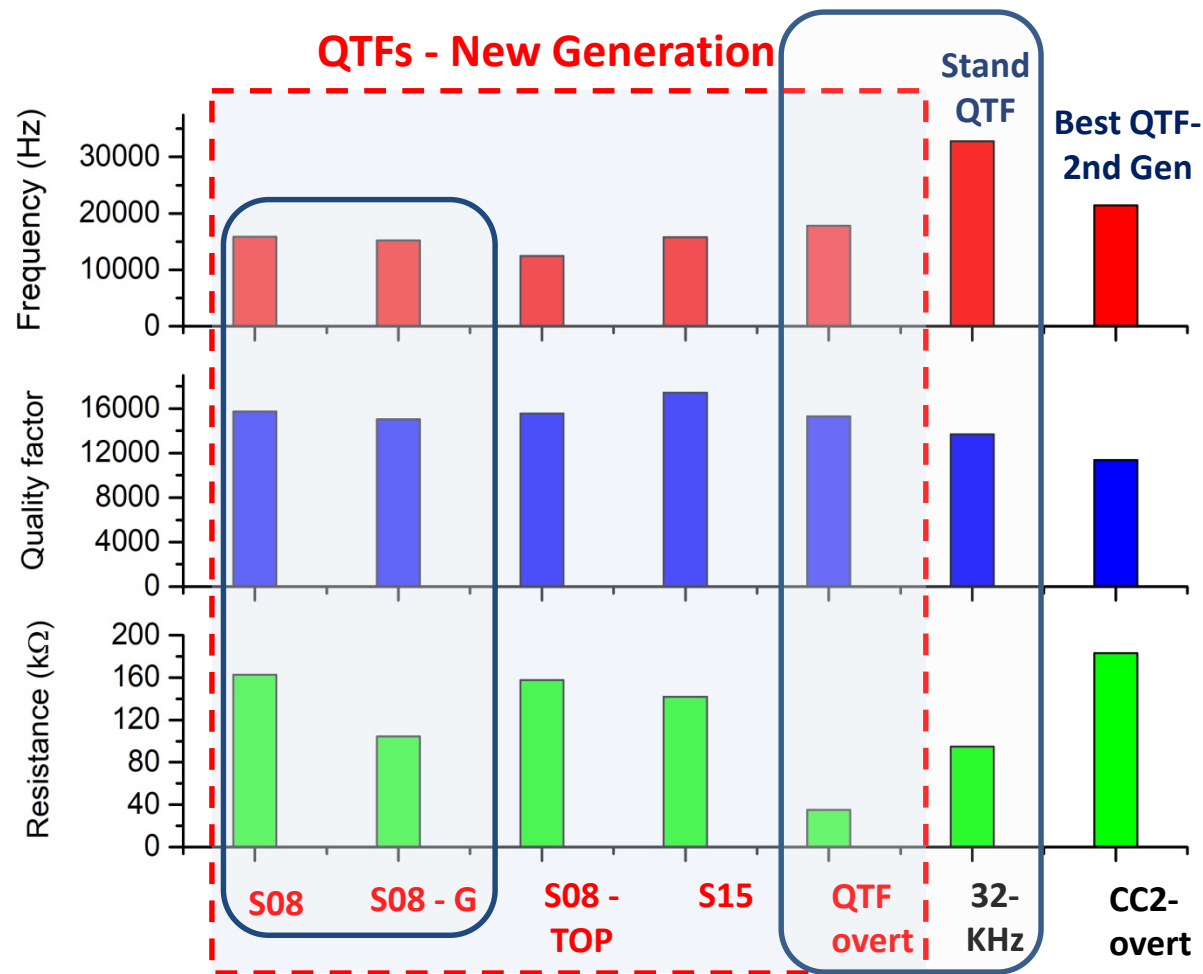
3rd gen. QTFs Electrical Characterization



Results are compared with a *standard 32 kHz-QTF* and the best QTF of the 2nd generation (*C-C2, overtone*)

- The **frequency was decreased by a factor of 2** with respect to the 32 KHz-QTF achieving **higher quality Q-factors**.
- Engraving **grooves** on the prongs surface **decreased the QTF electrical resistance by a factor of 2** (see S08-G vs S08).

3rd gen. QTFs Electrical Characterization



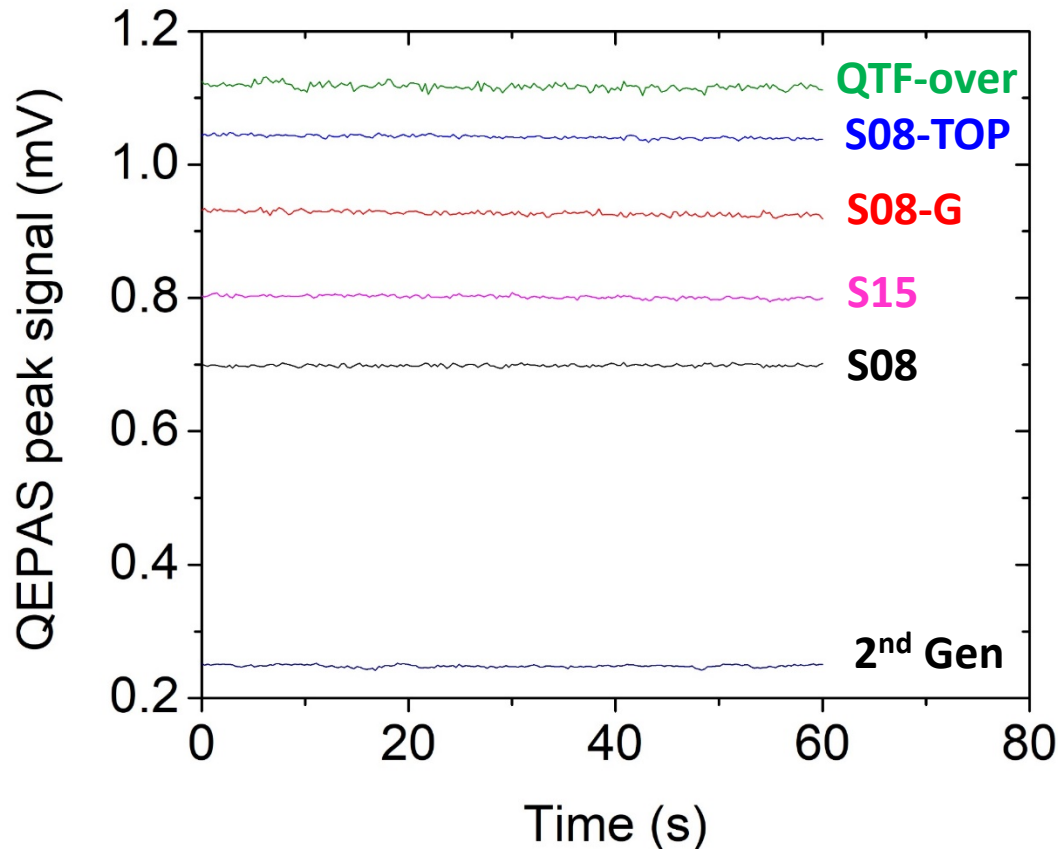
Results are compared with a *standard 32 kHz-QTF* and the best QTF of the 2nd generation (*C-C2, overtone*)

- The **frequency was decreased by a factor of 2** with respect to the 32 KHz-QTF achieving **higher quality Q-factors**.
- Engraving **grooves** on the prongs surface **decreased the QTF electrical resistance by a factor of 2** (see S08-G vs S08).
- The QTF operating in the **overtone mode (QTF-overt)** exhibits a **lower electrical resistance** than a 32KHz-QTF.

3rd gen. QTFs –Photoacoustic performances

Detection of a water line @7.7 μm , atm pressure

QEPAS line-locking measurements



All new QTFs show higher QEPAS signals than the 2nd generation.

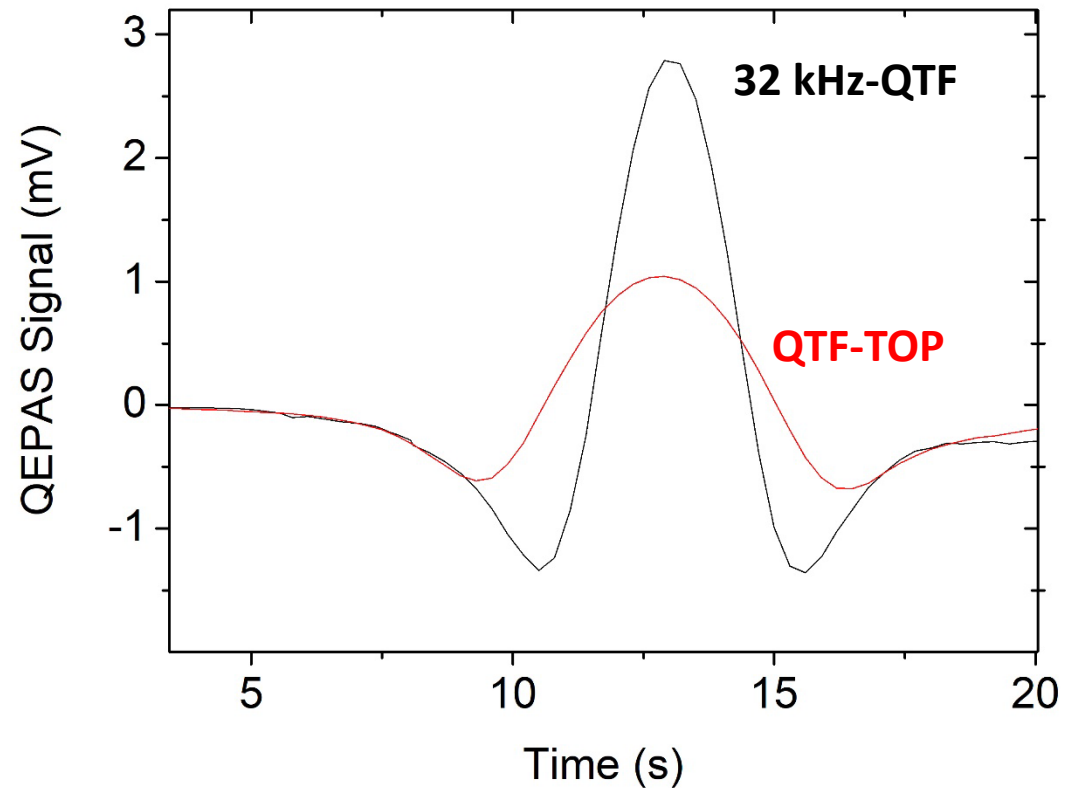
The noise level is nearly the same for all QTFs except for QTF-overtone, due to its narrower prongs spacing (700 μm).

3rd gen. QTFs – Comparison with 32 kHz-QTF

Detection of a water line @7.7 μm , atm pressure

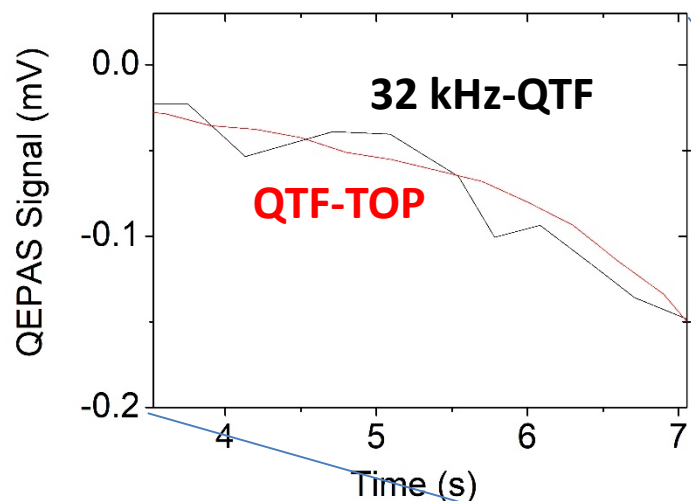
32 kHz-QTF exhibits a higher signal

QEPAS spectral scan measurements



3rd gen. QTFs – Comparison with 32 kHz-QTF

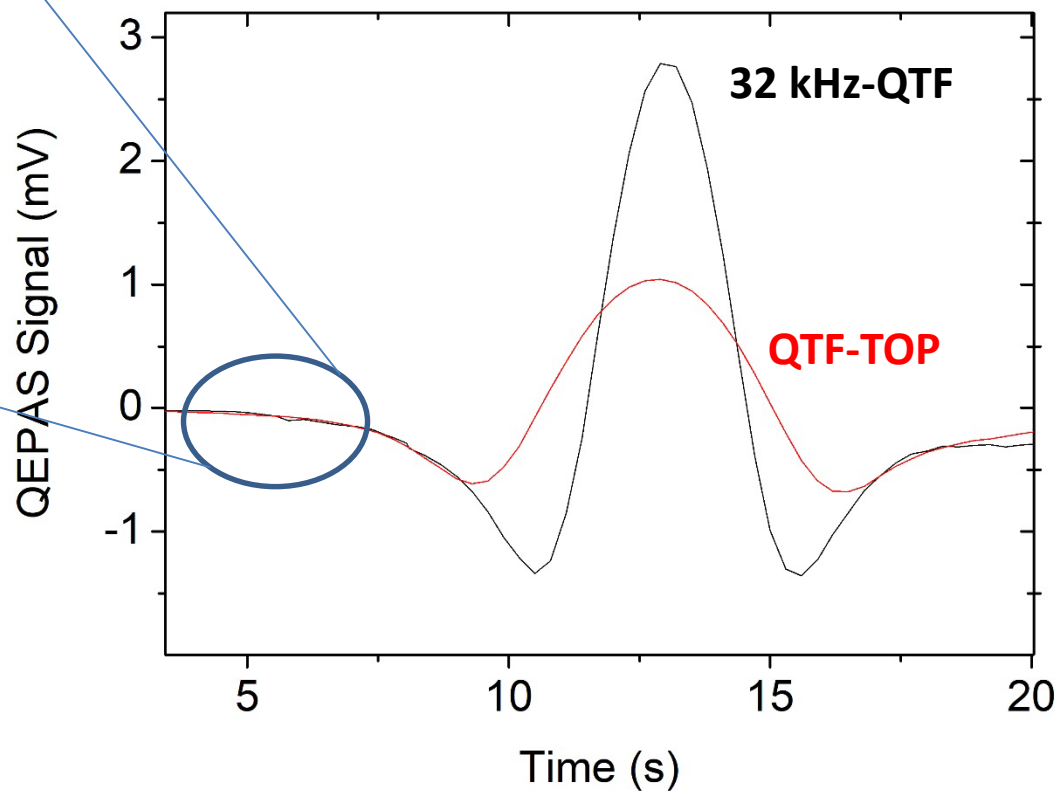
Detection of a water line @7.7 μm , atm pressure



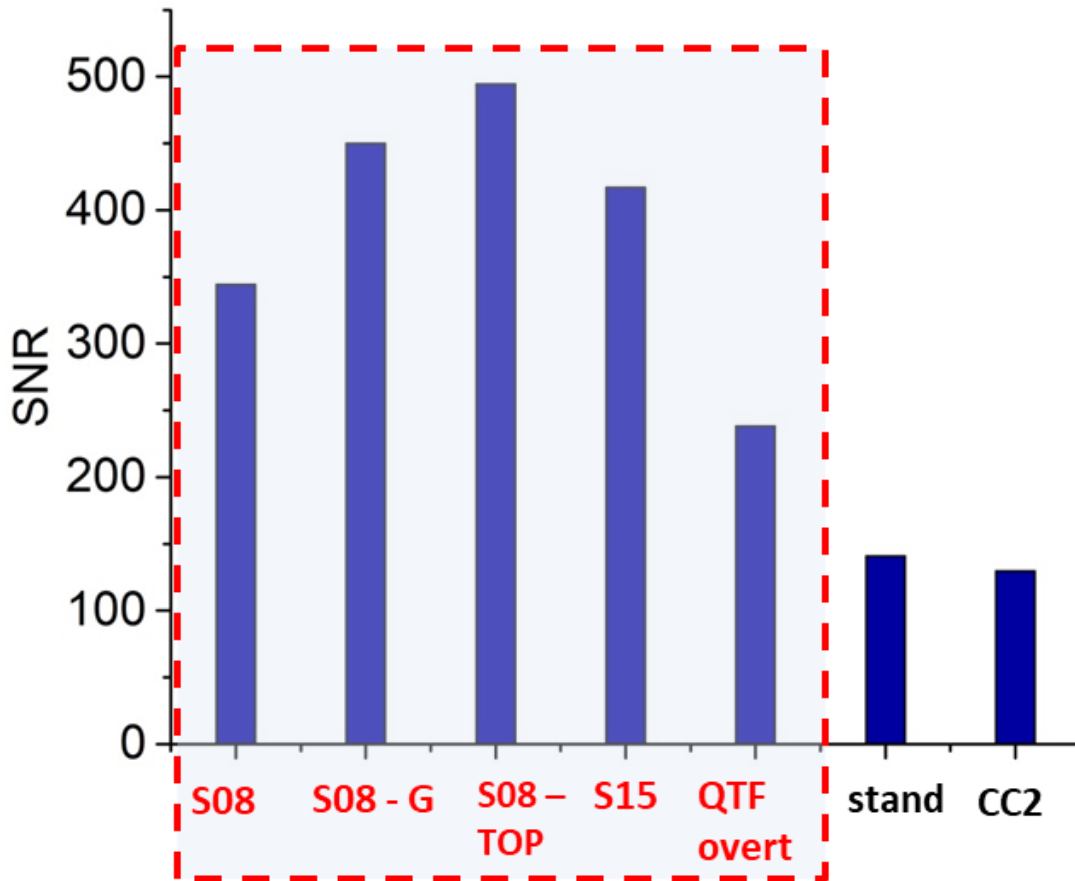
32 kHz-QTF exhibits a higher signal

but also a higher noise background

QEPAS spectral scan measurements



3rd gen. QTFs –SNR performances



All 3rd gen. QTFs exhibit **higher performance (SNR)** with respect to the 2nd gen. QTFs and the standard 32kHz QTF.

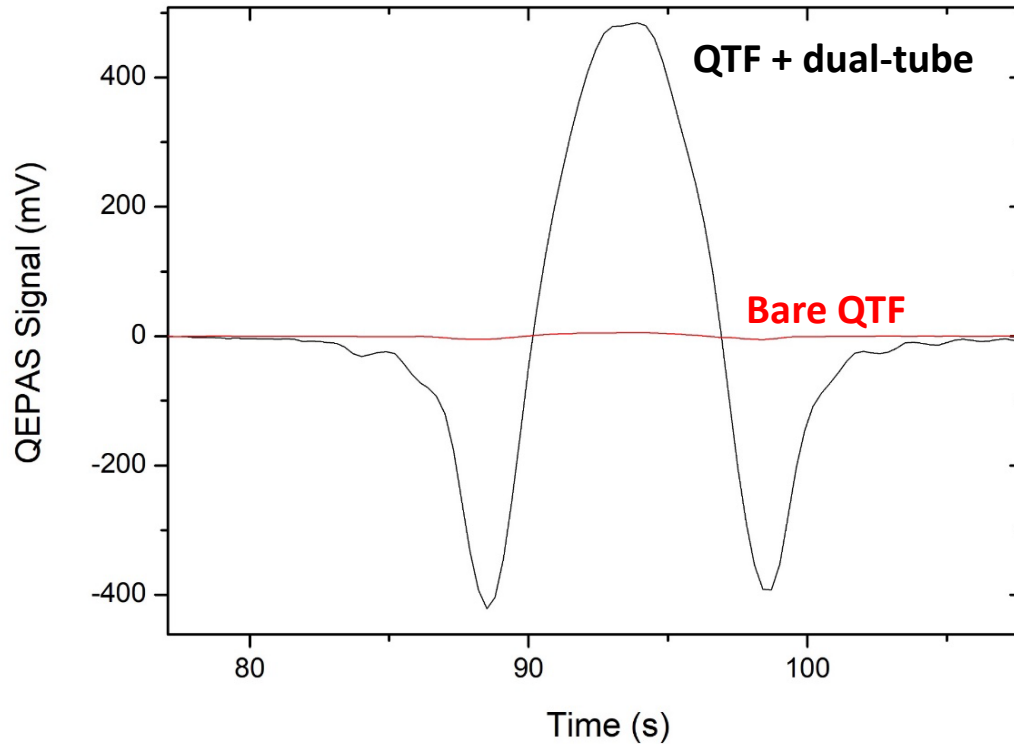
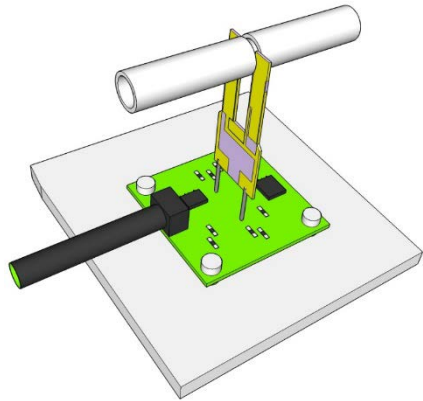
P. Patimisco et al, IEEE T. Ultr. Ferr., 65, 1951-1957,

2018
P. Patimisco et al, Optics Express 27, 1401-1415,

2019

QTF-S08-TOP with dual-tube resonator

ID = 1.59 mm and L = 12.4 mm



SNR Enhancement x60 (new QEPAS record)

New QEPAS Acoustic Detection Module with 3rd gen. QTF—available in the market in 2019



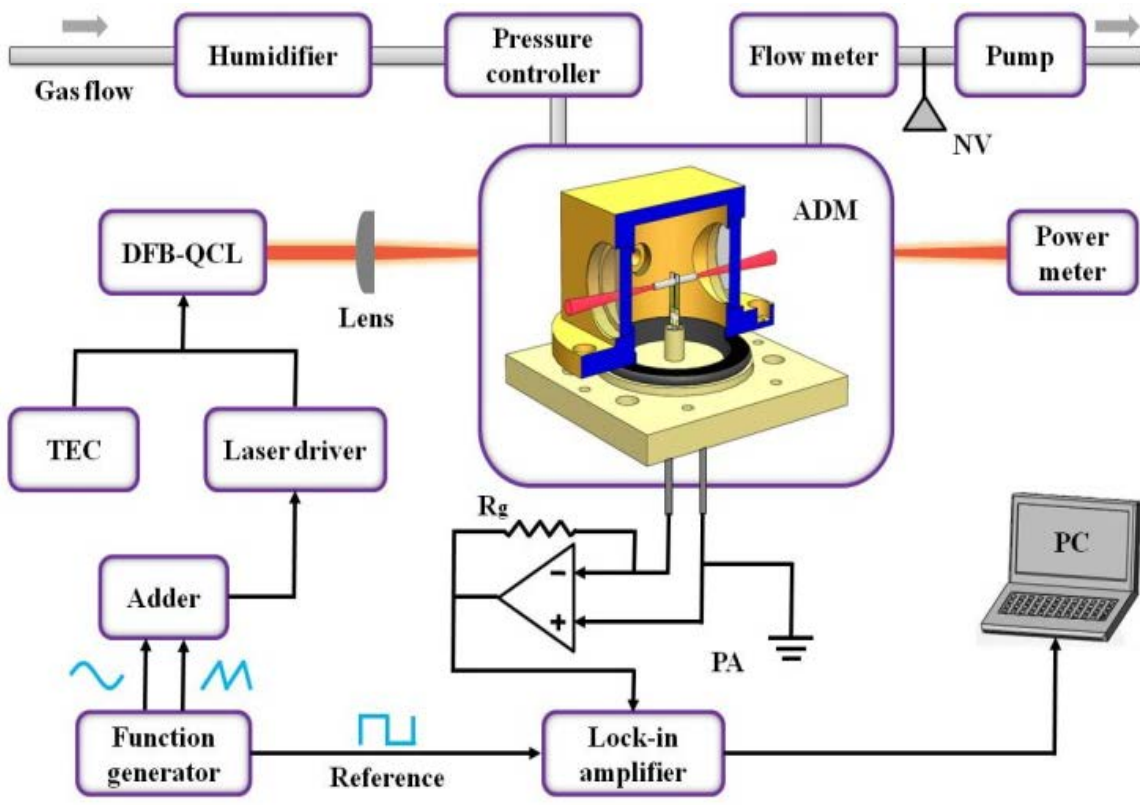
THORLABS

OUTLINE

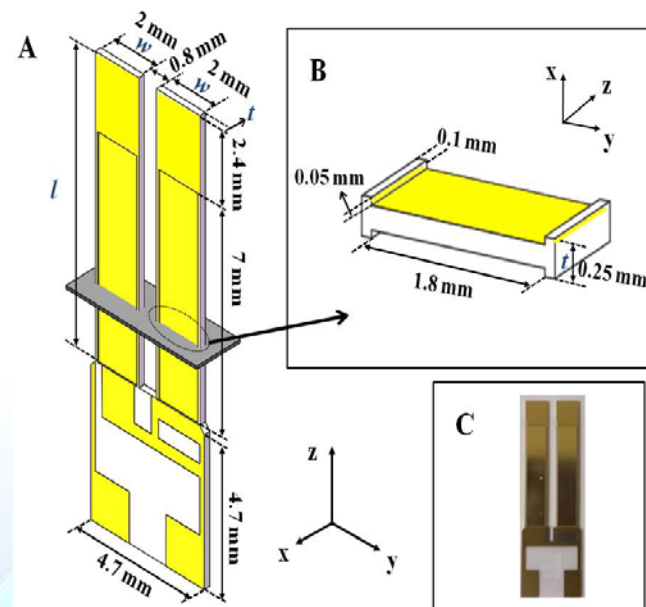


- Motivation for Gas Sensing
- Quartz Enhanced Photoacoustic Gas Detection
- QEPAS: Basic principles and merits
- QEPAS with custom quartz tuning forks
- QEPAS in the THZ range
- **Real world applications**

Carbon Oxide detection with 3rd gen QTF



QTF-S08-G



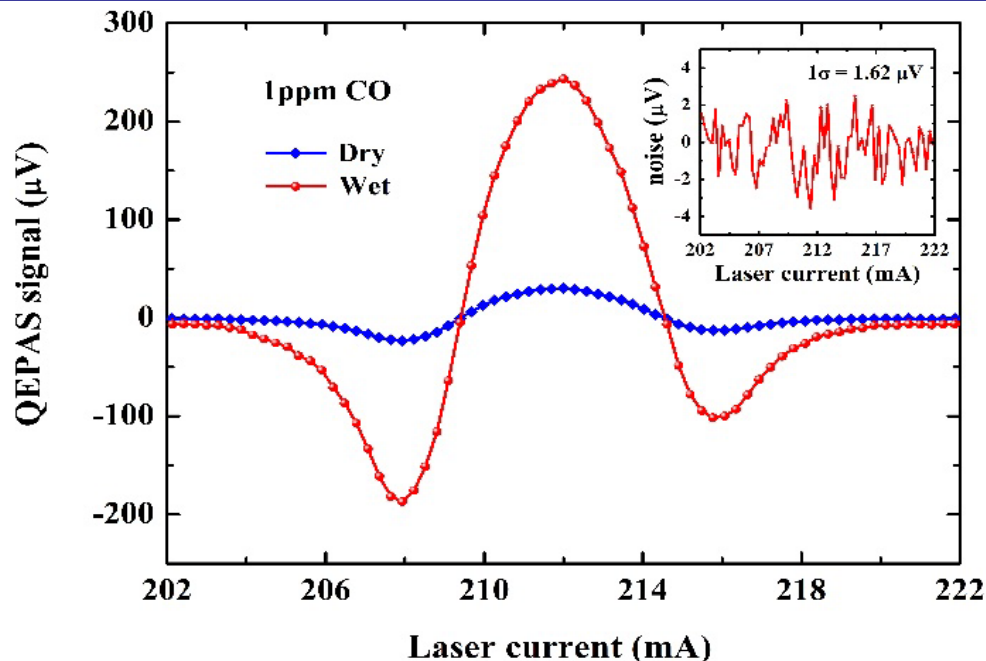
DFB-QCL emitting @ 4.61 μm

Optical power: 21 mW

Absorption line-strength: $4.5 \cdot 10^{-19}$ cm/mol

S. Li, L. Dong, H. Wu, A. Sampaolo, P. Patimisco, V. Spagnolo, F.K. Tittel, ACS Analytical Chemistry, *submitted 2019*

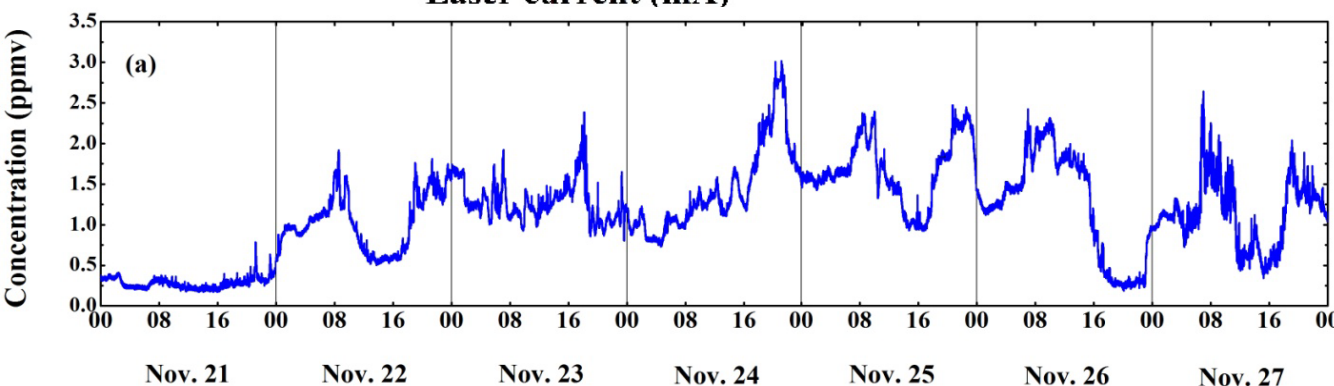
CO QEPAS Sensor calibration and detection limit



MDL: 7 ppb
with a 1 s integration time
QEPAS record for CO!

NNEA: $8.7 \cdot 10^{-9} \text{ cm}^{-1}\text{W} / \sqrt{\text{Hz}}$

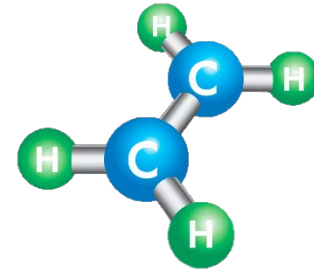
Continuous monitoring of atmospheric carbon oxide concentrations measured for a 7-day period in Nov. 2018 at Shanxi University, China



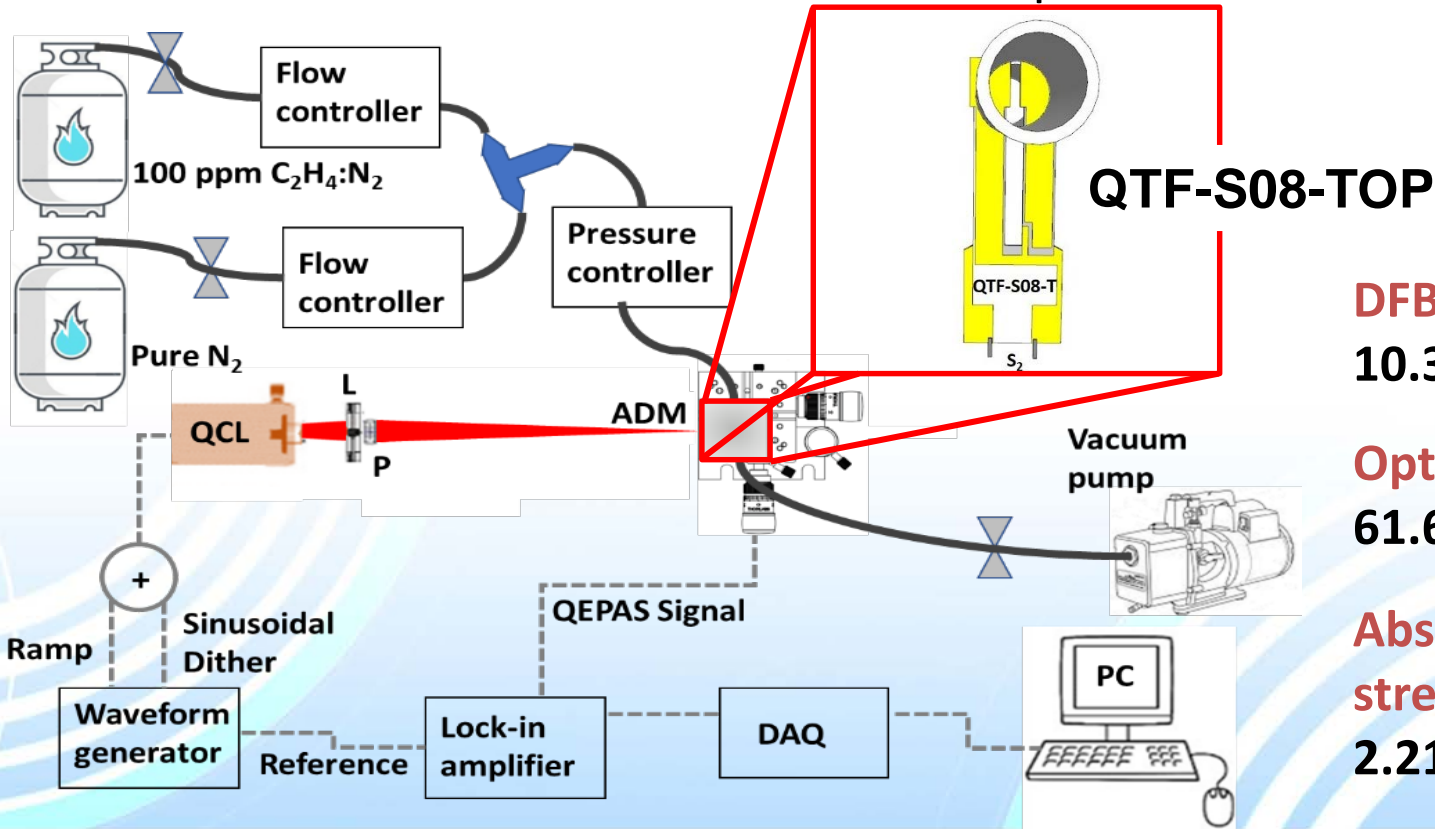
S. Li, L. Dong, H. Wu, A. Sampaolo, P. Patimisco, V. Spagnolo, F.K. Tittel, ACS Analytical Chemistry, *submitted 2019*

PolySenSe

Ethylene detection with 3rd gen QTF



- In chemistry, C_2H_4 is the basic building block for **hydrocarbons**
- **Breath biomarker** for bacterial infections
- **Plant hormone** associated with cellular respiration in fruits

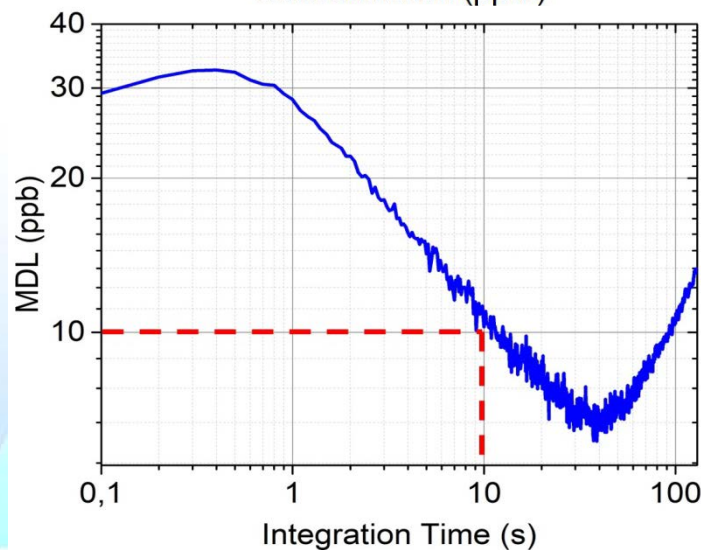
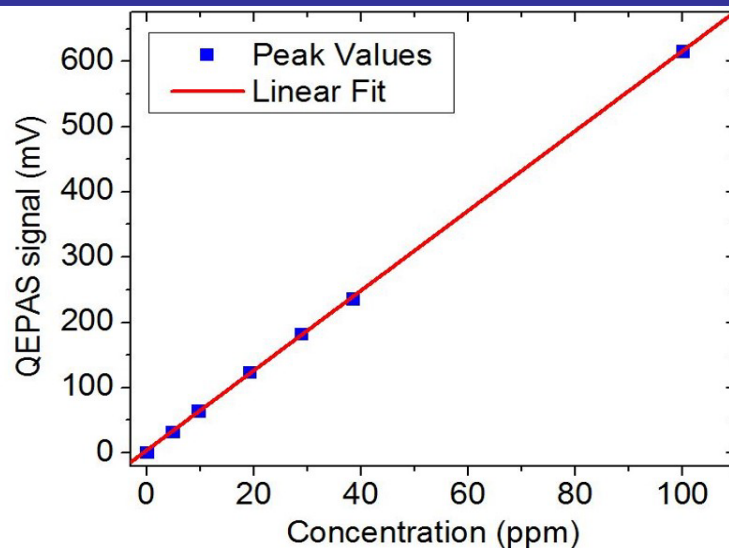
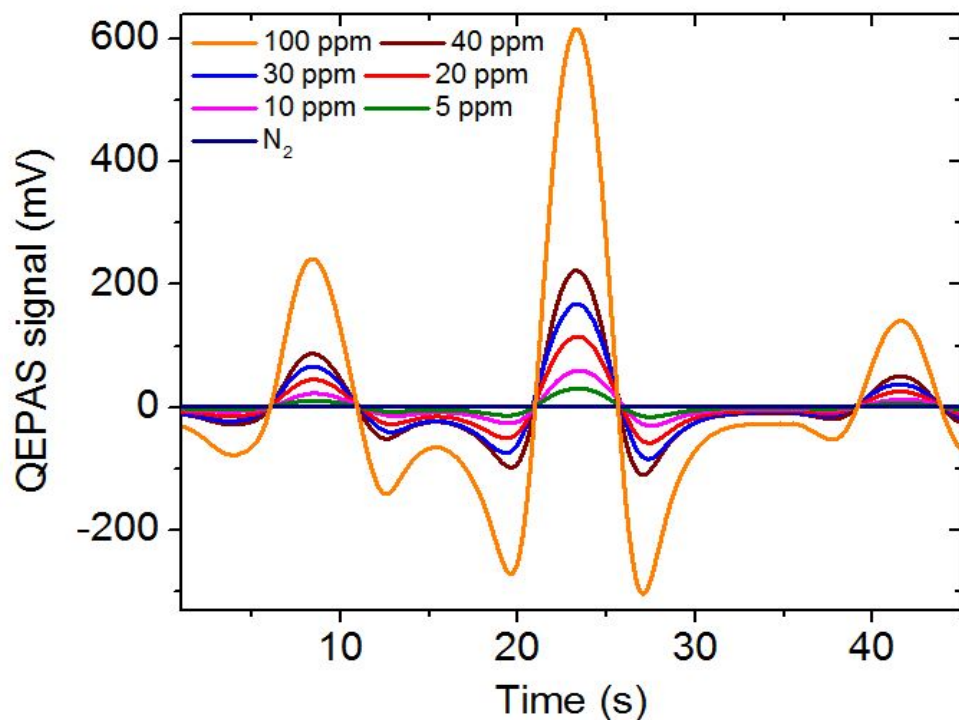


DFB-QCL emitting @
10.34 μm

Optical power:
61.6 mW

Absorption line
strength:
 $2.21 \cdot 10^{-20}$ cm/mol

C₂H₄ QEPAS Sensor calibration and detection limit



MDL: 29 ppb

with 100 ms integration time

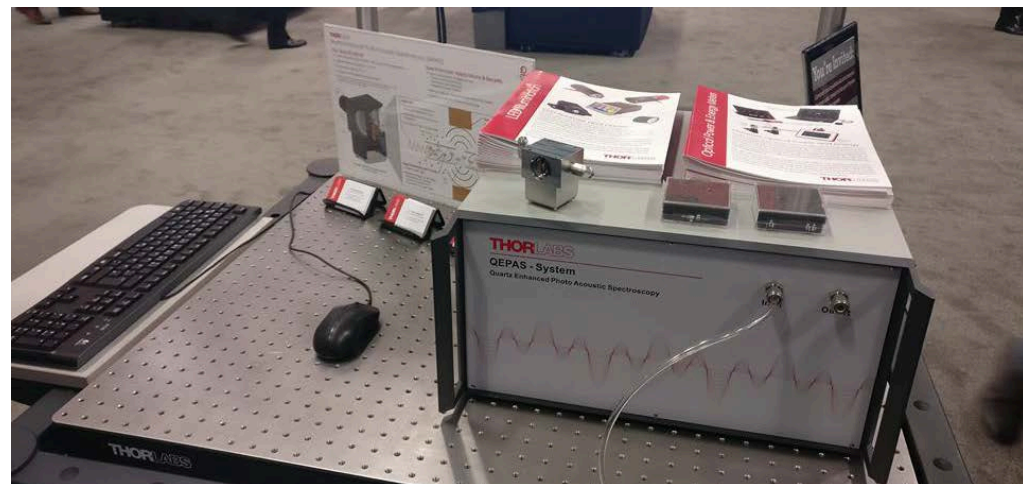
MDL: 10ppb

with 10 s integration time

QEPAS record for C₂H₄!

G. Marilena et al., Optics Express 27, 4271-4280, 2019

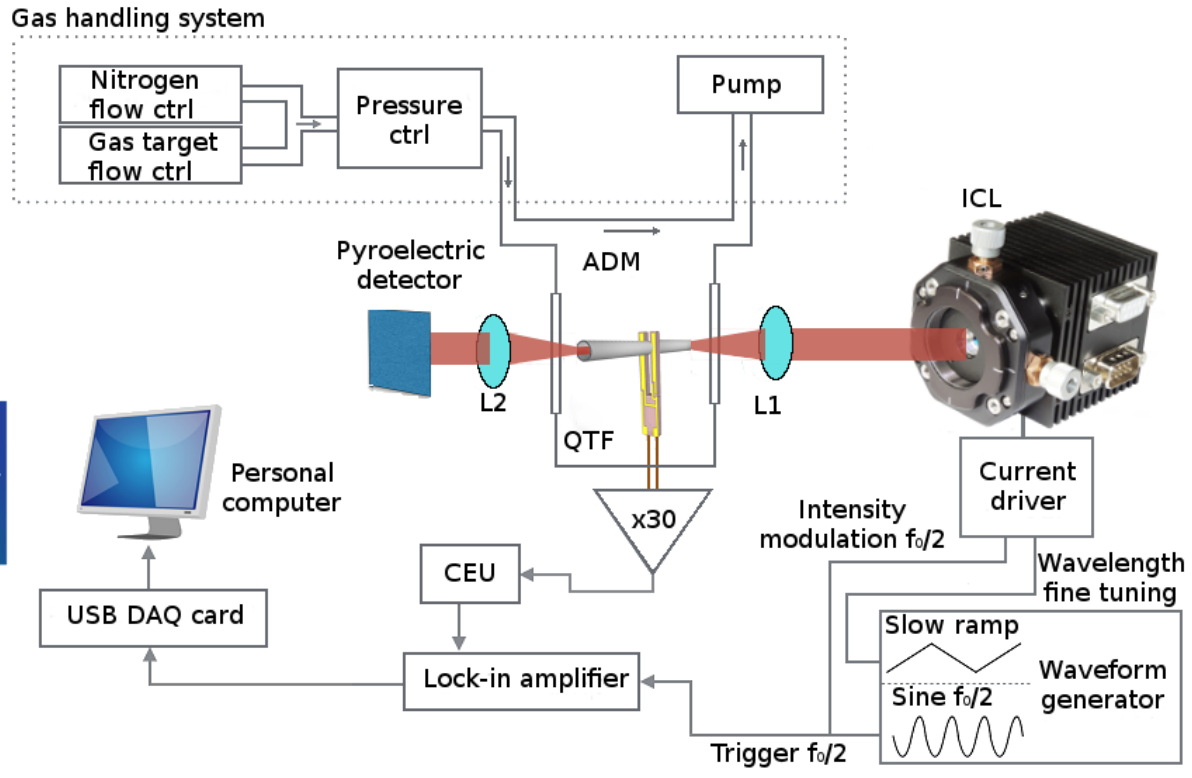
First commercial Ethylene QEPAS prototype Thorlabs Booth at Photonics West Feb. 2018



QEPAS Sensor setup for C1-C2-C3 detection

ILC characteristics

- $\lambda_{\text{emission}}$: **3345 nm**
- Tuning range: **12 nm**
- Optical Power: **12 mW**



Aramco Services Company



Spectroscopic technique

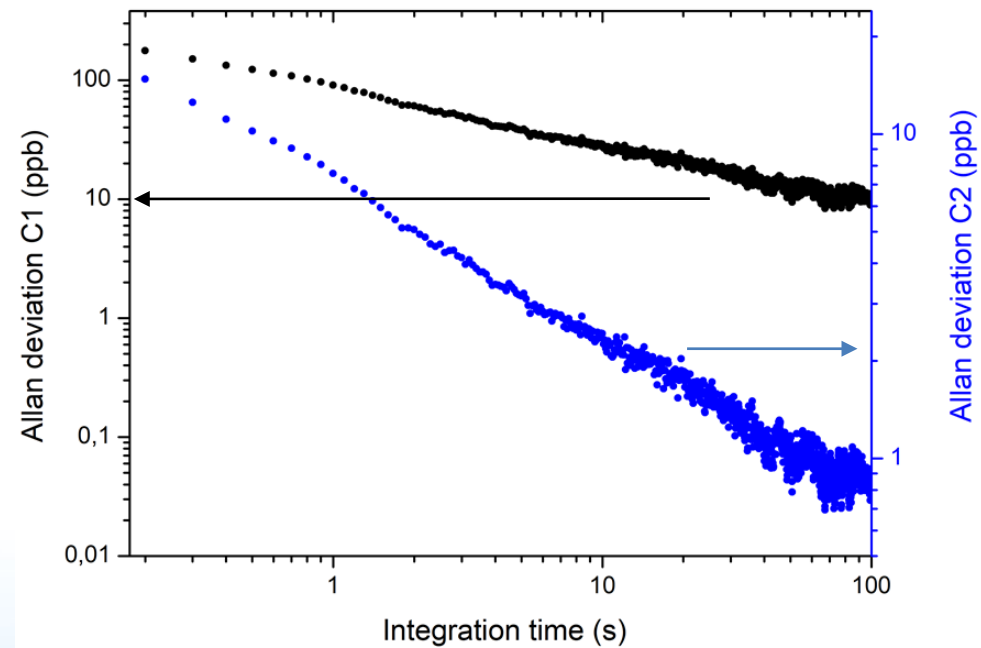
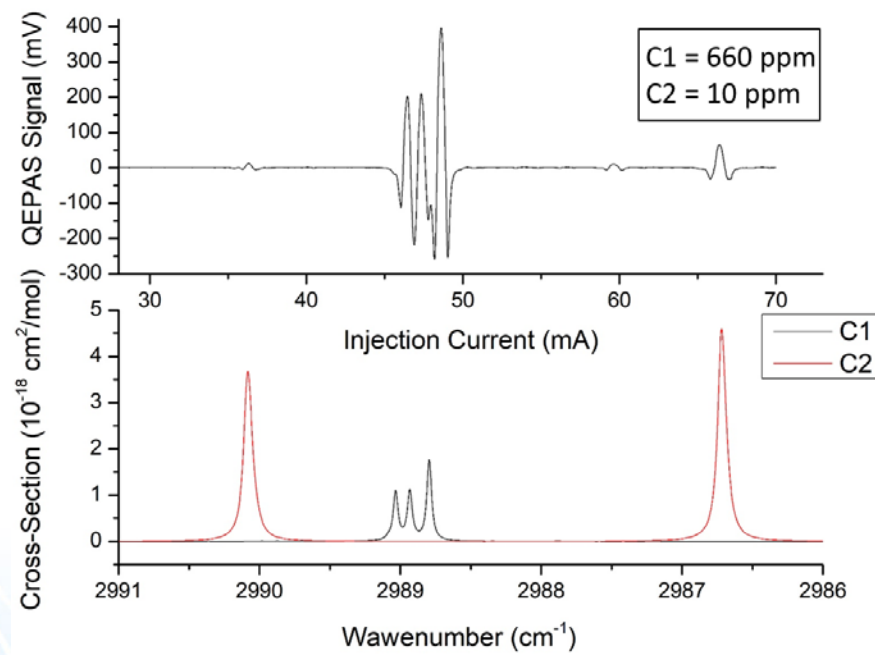
- **2f wavelength modulation**: laser current modulated at the half of the QTF resonance frequency and QEPAS signal demodulated by lock-in amplifier at the QTF resonance frequency → **background free detection**



Aramco Services
Company

Hydrocarbons QEPAS Sensor

C1-C2 detection



- Detection limit C1: **90 ppb** @ integration time **1 s**
- Detection limit C2: **7 ppb** @ integration time **1 s**,
RECORD for QEPAS technique



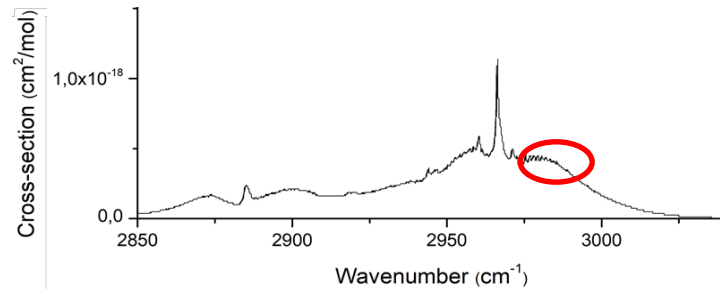
Hydrocarbons QEPAS Sensor

C2-C3 detection

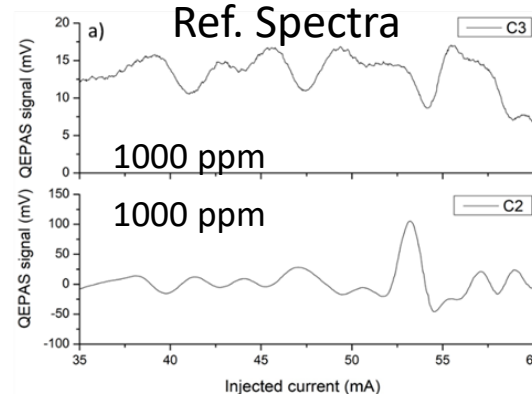
Aramco Services
Company



Propane absorption



$$Y(\lambda) = \sum_{i=0}^n A_i X(\lambda)_i = A_2 X(\lambda)_{C2} + A_3 X(\lambda)_{C3}$$



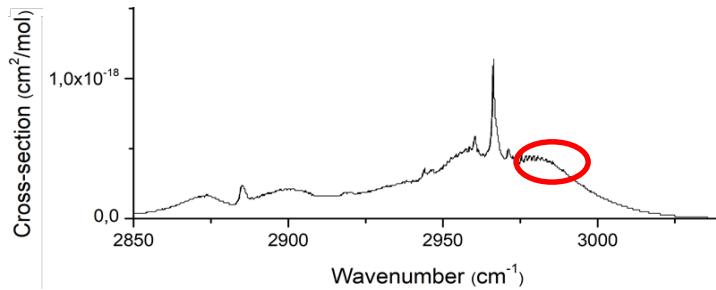
a) 2f-signal for 1000 ppm-C3 and 1000 ppm-C2 respectively in pure N₂



Hydrocarbons QEPAS Sensor

C2-C3 detection

Propane absorption

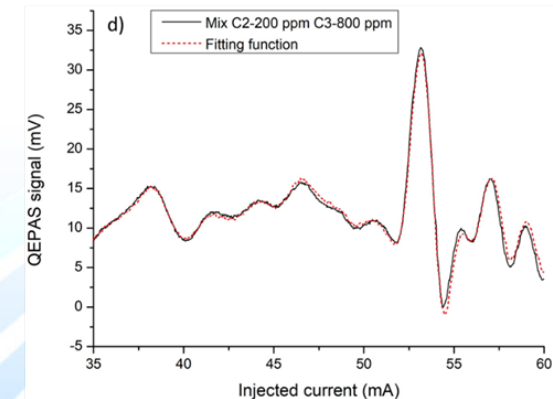
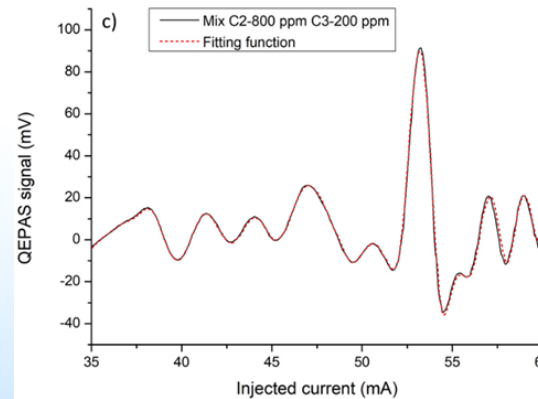
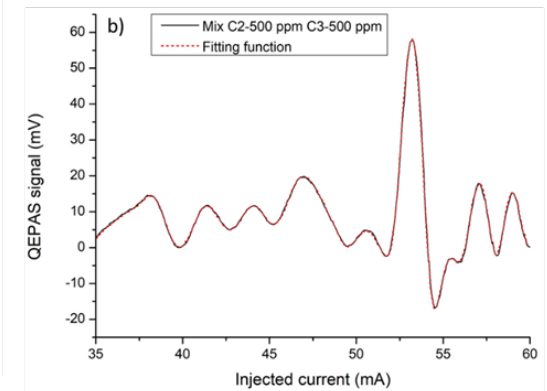
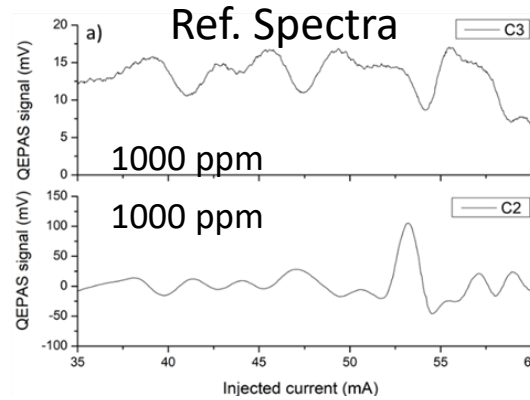


$$Y(\lambda) = \sum_{i=0}^n A_i X(\lambda)_i = A_2 X(\lambda)_{C2} + A_3 X(\lambda)_{C3}$$

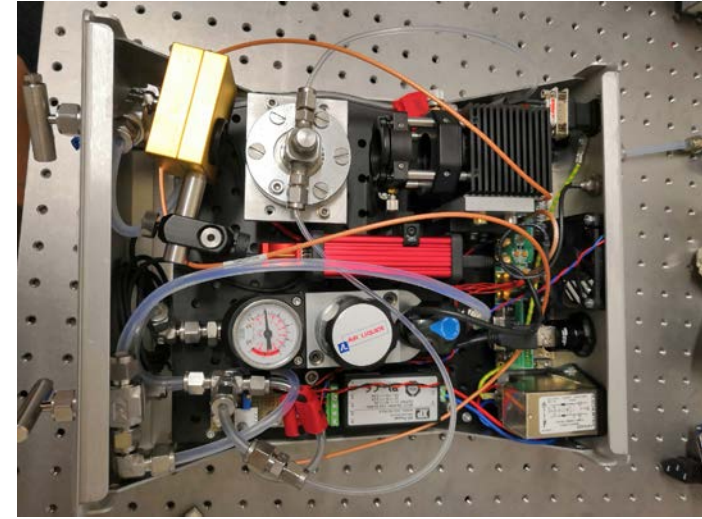
Mix	Actual C2 concentration [ppm]	Actual C3 concentration [ppm]	Calculated C2 concentration [ppm]	Calculated C3 concentration [ppm]
1	500	500	487.02 (±1.4)	520.00 (±2.5)
2	800	200	828.98 (±3.8)	208.01 (±6.8)
3	200	800	199.98 (±1.7)	831.47 (±2.9)

C3 detection limit @ 1s for peak at 5°C is 3 ppm

a) 2f-signal for 1000 ppm-C3 and 1000 ppm-C2 respectively in pure N₂; b) 2f-signal for a dry mixture containing 500 ppm of C2 and 500 ppm of C3, in pure N₂; c) 2f-signal for a dry mixture containing 800 ppm of C2 and 200 ppm of C3 in pure N₂; d) 2f-signal for a dry mixture containing 200 ppm of C2 and 800 ppm of C3 in pure N₂.



New QEPAS sensor system for hydrocarbon (C1, C2, C3) detection to be tested in Dahrán Spring 2019



2 kg

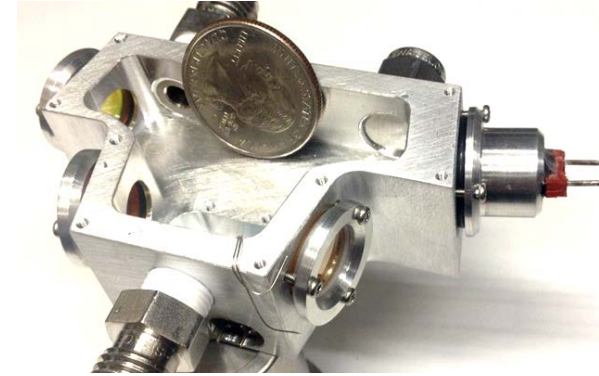
30cm x 10cm x 20cm

THORLABS

aramco 

Future Perspectives

- Realization of *QTFs 3rd generation*
- Develop ultra compact I-QEPAS sensors for high-sensitive detection
- Develop QEPAS sensors for mainstream, upstream and downhole petrochemical applications
- Develop QEPAS-on drone sensing systems
- Push QEPAS sensor systems development for *real-world applications* and *commercialization*



THORLABS

PolySense

**Aramco Services
Company**



Thank You



PolySenSe Team

Vincenzo Spagnolo
Pietro Patimisco
Angelo Sampaolo
Marilena Giglio
Giansergio Menduni
Arianna Elefante
Stefano Dello Russo
Fabrizio Sgobba
Andrea Zifarelli



THORLABS

Alex Cable
Bruno Gross
Verena Mackowiak
Hubert Rossmadl
Christian Brehm
Eric Geoffrion



INO-CNR
ISTITUTO
NAZIONALE DI
OTTICA

Simone Borri
Paolo De Natale



Rice University

Frank K. Tittel



Shanxi University

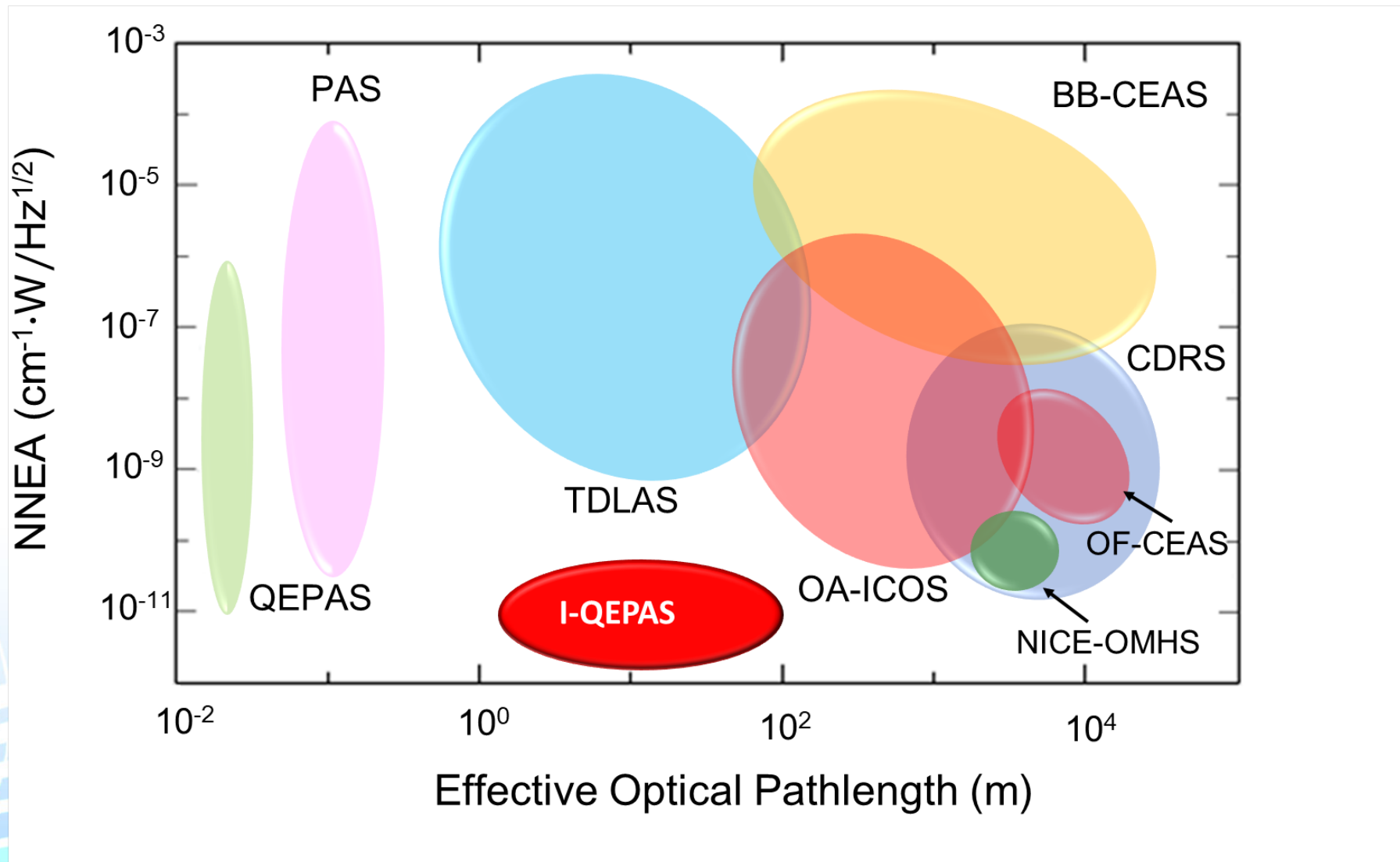
Lei Dong
Hongpeng Wu



Aramco Services
Company

Max Deffenbaugh
Sebastian Csutak

I-QEPAS vs Other Techniques



Design considerations for:

QTF-S15

Same geometry as QTF S08

Increased prong spacing up to 1.5 mm to:

- **Facilitate the optical alignment** of the focused laser beam
- Employ laser source with **poor spatial beam** quality or emitting in the **THz range**
- Implement micro-resonator tubes with **large inner diameters**
- **Investigate** of the influence of the **prongs spacing** on the QEPAS signal

QTF S15
(prongs spacing 1.5 mm)



P. Patimisco et al, IEEE T. Ultr. Ferr., 65, 1951-1957,
2018

P. Patimisco et al, Optics Express, *submitted*,

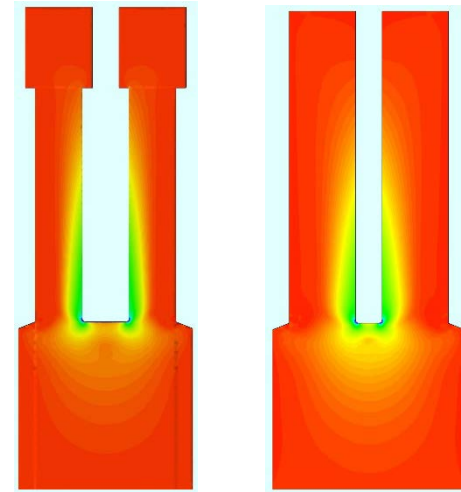
Design considerations for:

QTF-S08-TOP

Same geometry as QTF S08 but with a **wider top end** of on both prongs to **better distribute the stress field** along the prongs and increase the **generated piezo-charges**



QTF S08
TOP



QTF S08

QTF-S15

Same geometry as QTF S08

Increased prong spacing up to 1.5 mm to:

- **Facilitate the optical alignment** of the focused laser beam
- Employ laser source with **poor spatial beam** quality or emitting in the **THz range**
- Implement micro-resonator tubes with **large inner diameters**
- **Investigate** of the influence of the **prongs spacing** on the QEPAS signal

QTF S15
(prongs spacing 1.5 mm)



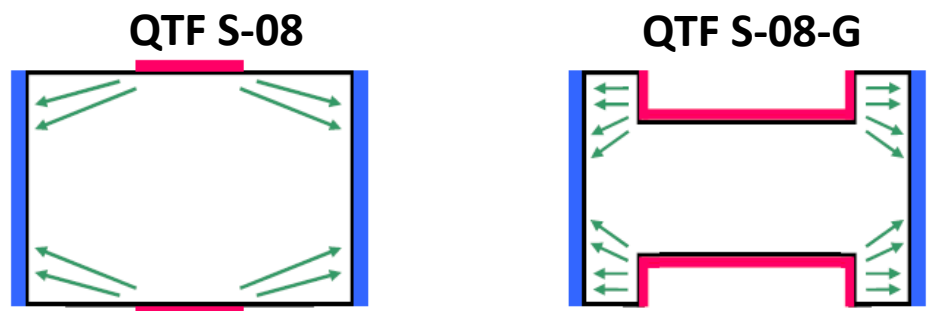
P. Patimisco et al, IEEE T. Ultr. Ferr., 65, 1951-1957,
2018

P. Patimisco et al, Optics Express, *submitted*,

Design considerations for QTF S-08-G

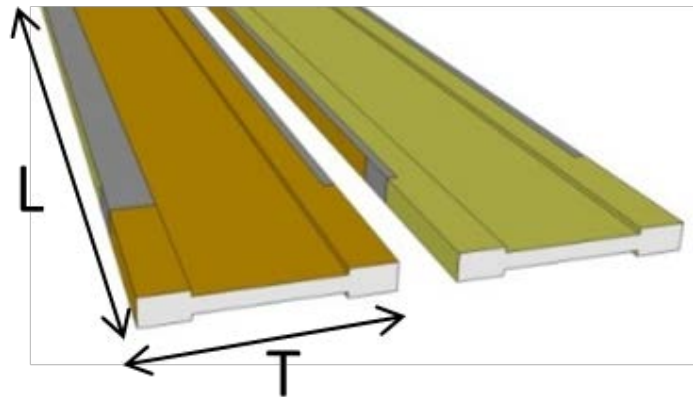
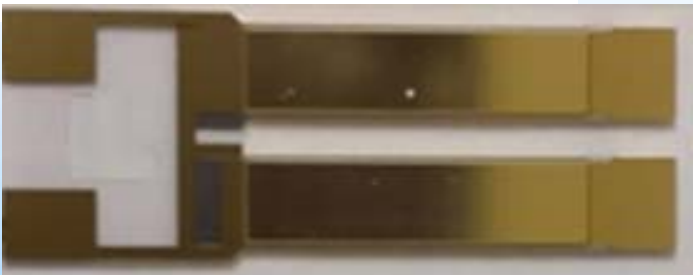
Same geometry of QTF S-08, but **with grooves** engraved on both surfaces of **the prongs** to reduce the electrical resistance

Top view of one prong



■ Positive Electrode
■ Negative Electrode
→ Electrical Field

QTF capacitance increases



$$C = \frac{1}{2\pi QRf}$$

Q and **f** depend on **T** and **L**
Not affected by grooves

R should be reduced

Higher **QEPAS signal**

Design considerations of QTF-overtone

QTF design optimized for **overtone mode** operation @ 17 kHz

Electrode layout designed to efficiently collect the generated **piezo-charges** (octupole configuration)

QTF-overtone
(prongs spacing 0.7 mm)

